New insights into Arctic paleogeography and tectonics from U-Pb detrital zircon geochronology

Elizabeth L. Miller,[1] Jaime Toro,[2] George Gehrels,[3] Jeffrey M. Amato,[4] Andrei Prokopiev,[5] Marianna I. Tuchkova,[6] Vyacheslav V. Akinin,[7] Trevor A. Dumitru,[1] Thomas E. Moore,[8] and Michael P. Cecile[9]

Received 11 April 2005; revised 21 December 2005; accepted 6 March 2006; published 6 June 2006.

[1] To test existing models for the formation of the Amerasian Basin, detrital zircon suites from 12 samples of Triassic sandstone from the circum-Arctic region were dated by laser ablation-inductively coupled plasma-mass spectrometry (ICP-MS). The northern Verkhoyansk (NE Russia) has Permo-Carboniferous (265–320 Ma) and Cambro-Silurian (410–505 Ma) zircon populations derived via river systems from the active Baikal Mountain region along the southern Siberian craton. Chukotka, Wrangel Island (Russia), and the Lisburne Hills (western Alaska) also have Permo-Carboniferous (280–330 Ma) and late Precambrian-Silurian (420–580 Ma) zircons in addition to Permo-Triassic (235–265 Ma), Devonian (340–390 Ma), and late Precambrian (1000–1300 Ma) zircons. These ages suggest at least partial derivation from the Taimyr, Siberian Trap, and/or east Urals regions of Arctic Russia. The northerly derived Ivishak Formation (Sadlerochit Mountains, Alaska) and Pat Bay Formation (Sverdrup Basin, Canada) are dominated by Cambrian–latest Precambrian (500–600 Ma) and 445–490 Ma zircons. Permo-Carboniferous and Permo-Triassic zircons are absent. The Bjorne Formation (Sverdrup Basin), derived from the south, differs from other samples studied with mostly 1130–1240 Ma and older Precambrian zircons in addition to 430–470 Ma zircons. The most popular plate tectonic model for the origin of the Amerasian Basin involves counterclockwise rotation of the Arctic Alaska–Chukotka microplate away from the Canadian Arctic margin. The detrital zircon data suggest that the Chukotka part of the microplate originated closer to the Taimyr and Verkhoyansk, east of the Polar Urals of Russia, and not from the Canadian Arctic.
Citation: Miller, E. L., J. Toro, G. Gehrels, J. M. Amato, A. Prokopiev, M. I. Tuchkova, V. V. Akinin, T. A. Dumitru, T. E. Moore, and M. P. Cecile (2006), New insights into Arctic paleogeography and tectonics from U-Pb detrital zircon geochronology, *Tectonics*, *25*, TC3013, doi:10.1029/2005TC001830.

1. Introduction

[2] Despite an increased interest in the exploration of the Arctic Ocean for both its resources and its role in controlling the Tertiary to recent climate history of Earth, we know remarkably little about the actual formation of this ocean basin and its changing paleogeography through time. Seafloor spreading anomalies constrain most of the rift history of the Eurasian Basin (the northern continuation of the Mid-Atlantic Ridge system) back to 56 Ma (anomaly 24) [e.g., *Rowley and Lottes*, 1988], but the earlier rift history of the adjacent Amerasian Basin (Figure 1) remains an unsolved plate tectonic puzzle. *Lawver and Scotese* [1990] chronicled the wide variety of solutions proposed for this puzzle over the years, and classified the solutions into three end-member rifting models where the Canadian Arctic margin and the Lomonosov Ridge are alternatively used as rift or transform boundaries for the displacement of Arctic Alaska, Chukotka and their continental shelves to their present position (Figure 1). Geophysical data sets and seismic reflection-based stratigraphic correlations have lent support to one of these rifting models, the "rotational opening model", often referred to as the "windshield wiper" model (Figures 1 and 2). This model proposes that Early Cretaceous rifting rotated a continental mass, now known as the Arctic Alaska-Chukotka microplate, southward from the Arctic margin of Canada. The plate pivoted about a pole located in the McKenzie Delta region [e.g., *Grantz et al.*, 1990b] (Figure 2), opening the Amerasian Basin by rifting. The Amerasian margin of the Lomonosov Ridge serves as a transform boundary in this model (Figures 1 and 2). Data in support of the "rotational model" include correlation of the upper Paleozoic-Mesozoic stratigraphy of the North Slope of Alaska to the Sverdrup Basin of Arctic Canada [*Grantz et*

[1]Department of Geological and Environmental Sciences, Stanford University, Stanford, California, USA.
[2]Department of Geology and Geography, West Virginia University, Morgantown, West Virginia, USA.
[3]Department of Geosciences, University of Arizona, Tucson, Arizona, USA.
[4]Department of Geological Sciences, New Mexico State University, Las Cruces, New Mexico, USA.
[5]Diamond and Precious Metal Geology Institute, Siberian Branch, Russian Academy of Sciences, Yakutsk, Russia.
[6]Geological Institute, Russian Academy of Sciences, Moscow, Russia.
[7]Northeast Interdisciplinary Scientific Research Institute, Russian Academy of Sciences, Magadan, Russia.
[8]U.S. Geological Survey, Menlo Park, California, USA.
[9]Geological Survey of Canada, Calgary, Alberta, Canada.

0278-7407/06/2005TC001830

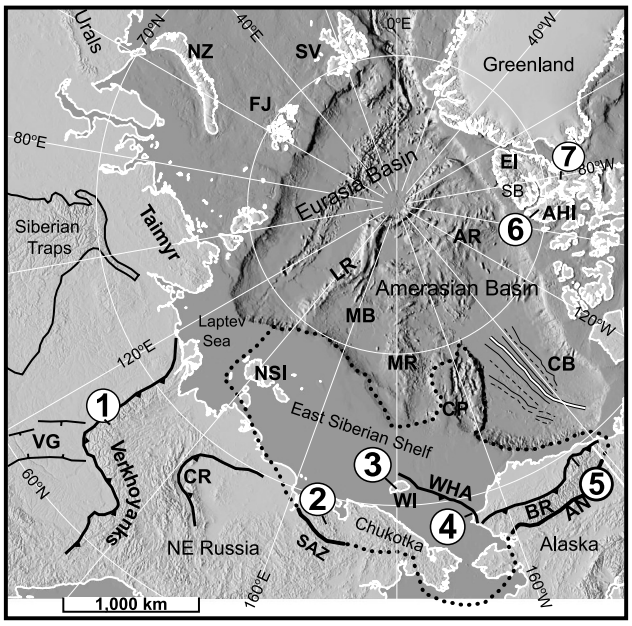

Figure 1. Circum-Arctic map showing the location of Triassic detrital zircon samples and the main tectonic features of the Arctic Basin. Bathymetry is from IBCAO (2001, available at http://www.ngdc.noaa.gov/mgg/bathymetry/arctic/arctic.html)). Sample locations are shown as numbered circles. See Table 1 for sample information and localities. The Arctic Alaska-Chukotka microplate is shown bounded by a heavy dotted line and as a solid line where ophiolitic rocks are exposed. The fossil spreading center for the Canada Basin is shown by a double line [*Laxon and McAdoo*, 1994] flanked by magnetic anomalies (positive, thin solid line; negative, thin dashed line). Abbreviations are AHI, Axel Heiberg Island; AN, Angayucham belt; AR, Alpha Ridge; BR, Brooks Range; CB, Canada Basin; CH, Chukotka; CP, Chukchi Plateau; Cr, Chersky Range; EI, Ellesmere Island; LR, Lomonosov Ridge; MB, Makarov Basin; MR, Mendeleev Ridge; NSI, New Siberian Islands; SAZ, South Anyui Zone; SB, Sverdrup Basin; SV, Svalbard; FJ, Franz Josef; VG, Vilyui Graben; WHA, Wrangel, Herald Arch; WI, Wrangel Island.

al., 1990b; *Embry and Dixon*, 1990; *Toro et al.*, 2004], and magnetic and gravity anomalies that identify a paleospreading center in part of the Amerasian Basin [*Laxon and McAdoo*, 1994; *Brozena et al.*, 2002]. Although the "rotational model" seems to best satisfy geological and geophysical data from the Canadian and Alaskan portion of the circum-Arctic, reconstructing the Russian portion of the Arctic Alaska-Chukotka plate by this model creates several problems. Geological and geophysical constraints suggest that the Arctic Alaska-Chukotka microplate extends as far west as the New Siberian Islands and includes most of the immense and poorly known east Siberian continental shelf (Figure 1) [*Kuzmichev and Soloviev*, 2004]. Restoring the microplate against the Canadian Arctic and Barents margins with the "rotational opening model" thus produces significant overlap of continental crust as discussed by *Rowley and Lottes* [1988], *Drachev* [2004], and *Natal'in* [2004] (Figure 2). Also, although the "rotational model" implies that the present-day southern margin of Arctic Alaska-Chukotka should have undergone shortening as the microplate rotated away from Arctic Canada, shortening in the Brooks Range appears to have started as early as mid-Jurassic [*Moore et al.*, 1994]. Therefore, if the Brooks Range belt of deformation extends into Chukotka, as is widely believed, the "rotational model" would juxtapose the trends of a mid-Jurassic–Early Cretaceous orogen against a platformal region with no such history (Figure 2), further calling this model into question.

[3] Understanding how the Amerasian Basin formed is necessary in order to understand the origin and evolution of the vast Russian continental shelves and basins as well as the origin of the major bathymetric features in the Arctic Ocean such as the continental Lomonosov Ridge, the more obscure Alpha-Mendeleev Ridge, and the Chukchi Borderland (Figure 1). At present, land-based geologic efforts provide the only straightforward and cost-effective means of addressing this problem. In particular, data from NE Russia has the most potential for making a significant contribution to our understanding. For instance, the reconstruction shown in Figure 2 suggests that Chukotka, Russia, should have depositional ties with Arctic Canada and not Siberia but this possibility has not been explored by land-based stratigraphic studies.

[4] Recent advances in laser ablation-mass spectrometry and ion microprobe technology have made the dating of large populations of detrital zircon feasible and now these methods are highly effective tools for provenance studies [e.g., *Dickinson and Gehrels*, 2003; *DeGraaf-Surpless et al.*, 2002]. The power of such studies for plate tectonic reconstructions is clear. Here we present U-Pb single-grain ages from detrital zircon populations of Triassic sandstones of the circum-Arctic, carried out in order to better constrain the position of the different parts of the Arctic Alaska-Chukotka microplate prior to the opening of the Amerasian Basin.

2. Arctic Alaska-Chukotka Microplate

[5] The key element in the plate tectonic evolution of the Amerasian Basin is the Arctic Alaska-Chukotka microplate. Figures 1 and 2 portray the microplate as a single elongate continental sliver. Figure 3 shows some of the salient aspects of its geology in more detail. Its northern boundary is the Arctic Alaskan and Russian outer shelf edges. Its southern boundary is defined by a belt of arc and ophiolitic rocks that includes the Angayucham terrane of the southern Brooks Range [e.g., *Moore et al.*, 1994] and the South Anyui zone of western Chukotka [e.g., *Seslavinskiy*, 1979; *Sokolov et al.*, 2002] (Figure 3).

[6] Arctic Alaska-Chukotka is believed to be a unified continental fragment because (1) Neoproterozoic volcanic and plutonic rocks with reported U-Pb zircon ages ranging from 750 to 550 Ma [*Moore et al.*, 1994; *Amato et al.*, 2003;

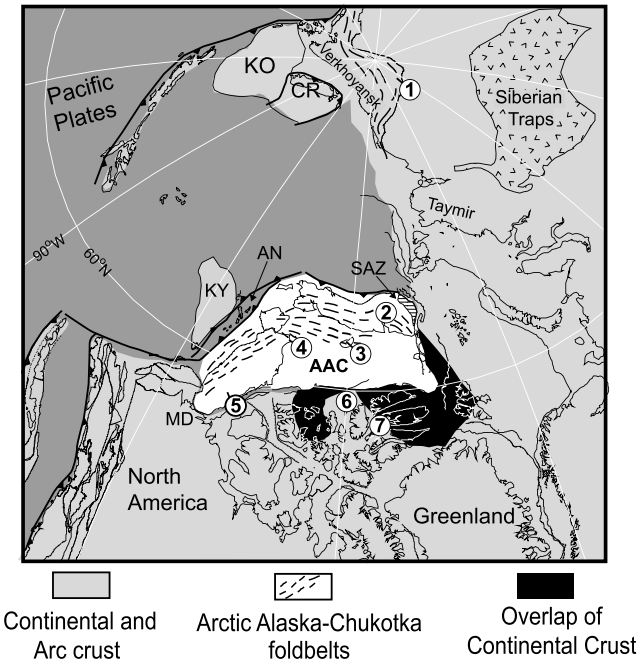

Figure 2. Early Cretaceous plate reconstruction of the circum-Arctic region prior to opening of the Amerasian Basin by simple rotation of Arctic Alaska-Chukotka (AAC) modified from *Lawver et al.* [2002]. The area of overlap of continental crust that results if AAC is rotated as a rigid plate is shown in black. The exposed area of the South Anyui Zone (SAZ) is highlighted by a ruled pattern. Numbered circles are detrital zircon sample locations. Abbreviations are AN, Angayucham belt; CR, Chersky range; KO, Kolyma-Omolon superterrane; KY, Koyukuk arc; MD, Makenzie Delta.

Amato, 2004, *Kos'ko et al.*, 1993] form its depositional basement; (2) Early Paleozoic carbonate successions with Siberian faunal affinities unconformably overlie this basement across its known extent [*Dumoulin et al.*, 2002; *Natal'in et al.*, 1999; *Kos'ko et al.*, 1993]; (3) the occurrence of a common suite of Devonian plutons (found in the Yukon, the Brooks Range, Seward Peninsula and Chukotka, with reported U-Pb ages ranging from 390 to 340 Ma [e.g., *Moore et al.*, 1994; *Toro et al.*, 2002; *Kos'ko et al.*, 1993]; and (4) the similar nature and age of structural trends across the microplate. These include ophiolite belts (the Angayucham and South Anyui) developed by collision-related deformation along the southern side of the plate and initiated in the mid-Jurassic, folds and thrust faults that involve continental margin sedimentary sequences from the Brooks Range and Lisburne Hills, where structures are well dated as latest Jurassic and Early Cretaceous, offshore along the Herald Arch to Wrangel Island, and into the Chukotka fold belt where shortening-related deformation is indirectly dated by syntectonic sedimentary sequences as latest Jurassic and Early Cretaceous [e.g., *Miller et al.*, 2004]. Structures are cut by Cretaceous plutons dated by the U-Pb method that are as old as 117 ± 1.9 Ma [*Katkov et al.*, 2004, 2005] (Figure 3). Volcanic sequences of the younger Okhotsk-Chukotsk belt in turn unconformably overlie older deformational structures and plutons [*Katkov et al.*, 2004, 2005] (Figure 3).

[7] One of the important along-strike differences in the stratigraphy of the microplate is the varying nature of Triassic sedimentary successions. Northern Alaska is characterized by a relatively thin, clastic passive margin succession, which includes chert and other pelagic deposits in the south and more proximal thin platform sandstones in the north. The Triassic succession of Alaska pinches out against a north-south trending basement high in the Chukchi platform east of Wrangel Island [*Sherwood et al.*, 2002] (Figure 3). In Chukotka, the Triassic consists of thick turbidite sequences intruded by gabbroic dikes and sills at their base [*Gelman*, 1963; *Ivanov and Milov*, 1975]. Sandstone petrography suggests recycled orogen sources [*Tuchkova et al.*, 2004]. Thus, in contrast to Alaska, Chukotka experienced a Triassic rifting event that formed deep basins across earlier platformal deposits and was paleogeographically linked to major immature clastic sources [*Tuchkova et al.*, 2004]. Deformation and metamorphism of the Triassic of Chukotka has hindered detailed studies of sedimentary facies and paleocurrents in these rocks and has obscured the initial geometry of these rift basins.

3. Analytical Methods

[8] Zircons were separated from 12 samples of Triassic sandstones (Table 1), mounted in epoxy and polished to expose the interior of the grains. Isotopic analyses were performed with a Micromass Isoprobe multicollector ICP-MS with a laser ablation system. Laser beam diameter was ~30 μm and yielded ablation pits ~20 μm deep. Grains were selected randomly from all sizes and morphologies present, except for avoidance of grains with fractures or inclusion. The ablated material is carried in argon gas into the plasma source of a Micromass Isoprobe, which is equipped with a flight tube of sufficient width that U, Th, and Pb isotopes are measured simultaneously. All measurements are made in static mode, using Faraday detectors for ^{238}U, ^{232}Th, ^{208}-^{206}Pb, and an ion-counting channel for ^{204}Pb. Ion yields are ~ 0.5 mv per ppm. Each analysis consists of one 20-s integration on peaks with the laser off (for backgrounds), twenty 1-s integrations with the laser firing, and a 30-s delay to purge the previous sample and prepare for the next analysis.

[9] Common Pb correction is made by using the measured ^{204}Pb and assuming an initial Pb composition from *Stacey and Kramers* [1975] (with uncertainties of 1.0 for ^{206}Pb/^{204}Pb and 0.3 for ^{207}Pb/^{204}Pb). Our measurement of ^{204}Pb is unaffected by the presence of ^{204}Hg because backgrounds are measured on peaks (thereby subtracting any background ^{204}Hg and ^{204}Pb), and because very little Hg is present in the argon gas.

[10] Interelement fractionation of Pb/U is generally ~15%, whereas fractionation of Pb isotopes is generally ~3%. In-run analysis of fragments of a large zircon crystal (generally every fourth measurement) with a known age of

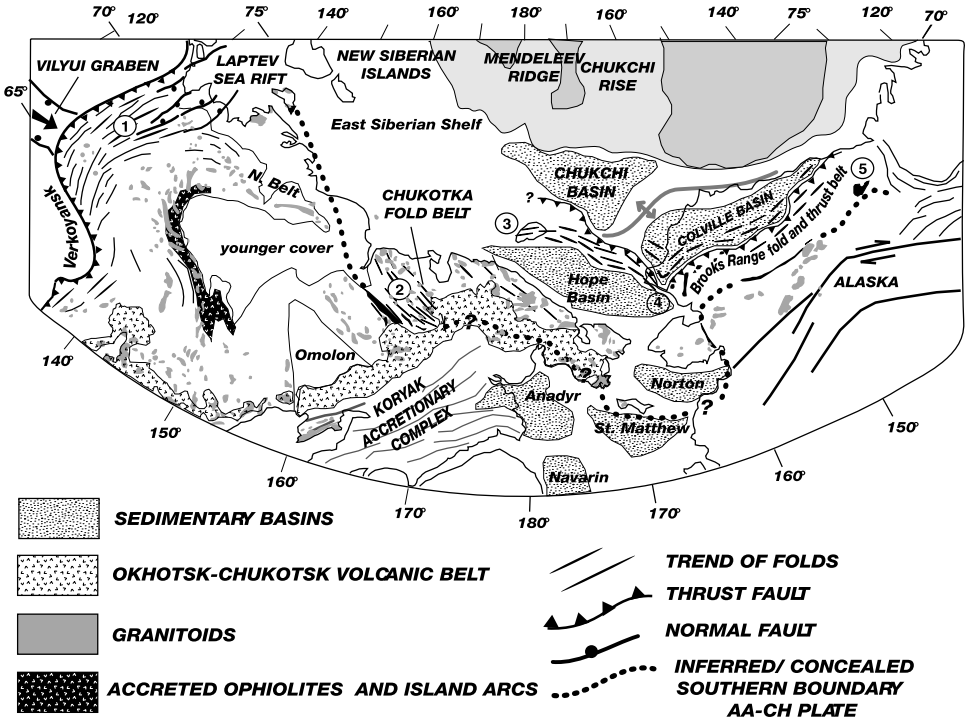

Figure 3. Tectonic map of the Arctic Alaska-Chukotka microplate illustrating key tectonic elements and geologic structures and relationships referred to in text.

564 ± 4 Ma (2-sigma error) [G. Gehrels, unpublished data] is used to correct for this fractionation. U and Th concentrations are calibrated by comparison with NIST SRM 610 trace element glass.

[11] The complete measured isotopic ratios and ages are reported in the auxiliary material Table S1.[1] Errors are from the measurement of $^{206}Pb/^{238}U$, $^{206}Pb/^{207}Pb$, and $^{206}Pb/^{204}Pb$ and are reported at the 1-sigma level. Additional errors that affect all ages include uncertainties from (1) U decay constants, (2) the composition of common Pb, and (3) calibration correction. These systematic errors add an additional 1–2% (1-sigma) uncertainty to $^{206}Pb/^{238}U$ and >1.0 Ga $^{206}Pb/^{207}Pb$ ages.

[12] Age interpretations for <1.0 Ga analyses are based largely on $^{206}Pb/^{238}U$ ages. $^{206}Pb/^{207}Pb$ ages for these analyses are much less reliable given the low concentration of ^{207}Pb. Because of this, discordance on an individual grain basis cannot be assessed for grains younger than 1.0 Ga.

[13] For grains >1.0 Ga, $^{206}Pb/^{207}Pb$ ages are generally more precise than $^{206}Pb/^{238}U$ ages, and are accordingly used in age interpretations. For the older grains, discordance can be assessed because both the $^{206}Pb/^{238}U$ and $^{206}Pb/^{207}Pb$ ages are measured reliably. However, it should be noted that $^{206}Pb/^{207}Pb$ ages underestimate the true age for discordant grains given that isotopic disturbance occurred in the geologic past. To reduce the effect of discordance, only analyses that are less than 20% discordant are included in age interpretations (applicable only to older grains). The interpreted ages are presented in Table 2.

[14] Most of the zircons analyzed are igneous in origin with U/Th < 3 (Figure 4). The U-Pb dates are plotted on relative age probability distribution diagrams [*Ludwig*, 2003]. The relative height of the peaks corresponds to the relative abundance of that population of ages (Figures 5 and 6). Some analyses were not plotted because of one of two reasons: (1) for ages <1000 Ma, the $^{206}Pb/^{238}U$ uncertainty was >10%, and (2) for ages >1000 Ma, the $^{207}Pb/^{206}Pb$ uncertainty was >10% or the discordance between the $^{206}Pb/^{238}U$ and $^{207}Pb/^{206}Pb$ ages was > 20%.

[15] We discuss the detrital zircon suites from the Triassic of Russia on a sample by sample basis (Figure 5), but we group these and other samples that have similar detrital zircon ages together in Figure 6 so that the characteristics of all localities studied can be compared to one another. To clarify the discussion of individual samples and to better allow comparison of data from different samples, a list of selected peak ages and the age ranges of grains characterizing those peaks is provided in Table 3. Criteria for this selection of peaks are listed at the end of Table 3.

4. Geological Setting of Samples and Interpretation of Detrital Data

[16] Triassic sandstones were selected for our study because they represent the youngest stage of widespread marine deposition prior to the onset of shortening and

[1] Auxiliary material is available at ftp://ftp.agu.org/apend/tc/2005tc001830.

Table 1. Sample Data for Sandstones Analyzed for Detrital Zircons

Field	Number on Figures	Area	Latitude	Longitude	Age	Unit
00JT25	1	Verkhoyansk	65.450207	126.897921	Middle Triassic	Tolbon Formation
00JT26	1	Verkhoyansk	65.438062	126.875138	Middle Triassic	Tolbon Formation
00JT29	1	Verkhoyansk	65.336460	126.343293	Upper Triassic	Khedalichen Formation
CH3.1B	2	Chukotka	67.868222	166.290222	Upper Triassic	Carnian T3k
CH2.6	2	Chukotka	68.061778	166.412000	Upper Triassic	Carnian T3k
CH26.5	2	Chukotka	69.156528	165.038222	Upper Triassic	Norian T3n
C145741	3	Wrangel Island	71.031667	179.216667	Triassic	Triassic Unit
94CL10	4	Lisburne Hills	68.868667	166.059667	Upper Triassic	Otuk Formation
94CL53	4	Lisburne Hills	68.861167	166.014667	Upper Triassic	Otuk Formation
96DH102	5	Sadlerochit Mountains	69.684330	144.849000	Lower Triassic	Ledge Member, Ivishak Formation
AE1	7	Sverdrup Basin	79.566667	83.333333	Lower Triassic (Smithian)	Bjorne Formation
AE2	6	Sverdrup Basin	80.583333	95.950000	Upper Triassic (Carnian)	Pat Bay Formation

subsequent rifting that led to the deformation and dispersal of terranes by formation of the Amerasian Basin. Crustal shortening affected parts of Arctic Alaska starting as early as the Middle Jurassic when arc-related ophiolitic sequences were emplaced northward in a deep water setting, south of the present-day Brooks Range [e.g., *Moore et al.*, 1994]. There is a striking similarity in the timing of ophiolite and arc emplacement in Alaska and the Kolyma region east of the Verkhoyansk (Figure 3), which also began to deform in the Middle Jurassic. [*Oxman et al.*, 1995] (see discussion by *Miller et al.* [2002]). The main period of folding and thrusting in the Brooks Range is dated by synorogenic deposits of the Okpikruak Formation of Late Jurassic to Early Cretaceous age, similar in age to synorogenic deposits of Chukotka [*Miller et al.*, 2004; *Katkov et al.*, 2005]. Localized rifting began in the Late Jurassic along the northern Alaskan margin (the Dinkum graben [*Grantz et al.*, 1990a]), but the major episode of seafloor spreading that formed the Amerasian Basin is believed to have taken place in the Early Cretaceous (*Grantz et al.* [1990b], but see *Drachev* [2004]). Widespread plutons across the Arctic Alaska-Chukotka plate (Figure 3) are everywhere believed to postdate collision-related deformation and the Angayucham and South Anyui belts. They are as old as 118 Ma and as young as 95 Ma and many are associated with vertical flattening and/or horizontal extensional fabrics [*Klemperer et al.*, 2002, *Miller et al.*, 2002, 2004; *Katkov et al.*, 2004, 2005], arguing for perhaps significant internal deformation of the Arctic Alaska-Chukotka plate during this time span.

[17] Detrital ages were measured in seven samples of Triassic sedimentary rocks collected along the length of the Arctic Alaska-Chukotka microplate to test both the structural integrity and stratigraphic continuity of this crustal fragment as well as to constrain paleogeographic links between Triassic sediments and their source areas. Three Triassic samples from the northern Verkhoyansk fold-and-thrust belt were analyzed to characterize the source regions for the NE Russian margin clastic wedge (which spans the Carboniferous to Early Jurassic) and two additional samples were dated from the Sverdrup Basin, Arctic Canada, to characterize the source for Triassic sandstones that presumably lay adjacent to Chukotka prior to rifting and rotation of the Arctic Alaska-Chukotka microplate away from the Canadian Arctic (Figures 1 and 2).

[18] Our data set (Figures 5 and 6) shows that nearly all of the Triassic sandstones analyzed were derived primarily from the erosion of Paleozoic and early Mesozoic source terranes. Precambrian zircons are present in all samples but in limited amounts, with the exception of one sample from the southern Sverdrup Basin (Figure 6). Our discussion below focuses on the interpretation of the Phanerozoic ages in the zircon populations because these are the most easily linked to possible source areas and thus are most useful for paleogeographic reconstructions. The three samples from the Russian Verkhoyansk margin and the three samples from Chukotka (Russia) are discussed first and in greater detail (Figure 5).

4.1. Northern Verkhoyansk (Locality 1)

[19] The shallow marine to nonmarine Triassic succession of the Verkhoyansk (Figure 3) is part of an immense passive margin siliciclastic wedge that ranges in age from Carboniferous to Early Jurassic [e.g., *Khudoley and Guriev*, 1994]. A major fluvial system (or systems) is thought to have connected the tectonically active Baikal Mountain region to the Verkhoyansk margin via the Vilyui graben system (Figures 1 and 3) and other similar distributary systems [e.g., *Khudoley and Guriev*, 1994].

[20] Earliest Triassic strata of the northern Verkhoyansk (the Nedshel and Tagand Formations) contain basalt flows and tuffs that are believed to be coeval with Permo-Triassic boundary Siberian Trap magmatism (for location, see Figure 1 and 3) [*Andrianova and Andrianov*, 1970] but were not analyzed as part of this study. Middle and Upper Triassic sandstones have petrographic characteristics of "recycled orogen" sources, compatible with their inferred provenance from the actively uplifting Baikal Mountains. They do not contain any Permo-Triassic zircons (Figure 5).

Table 2. Interpreted Zircon Ages[a]

Verkhoyansk			Chukotka		
00JT25	00JT26	00JT29	CH31B	CH26	CH265
256.0 ± 7.6	275.5 ± 7.3	269.2 ± 4.7	235.8 ± 10.5	240.0 ± 8.4	253.7 ± 1.6
274.6 ± 15.2	280.5 ± 8.6	272.7 ± 6.3	237.8 ± 2.6	246.2 ± 4.7	257.7 ± 9.4
291.7 ± 11.5	287.0 ± 12.2	285.5 ± 10.7	241.6 ± 7.4	251.4 ± 7.7	264.7 ± 8.8
295.8 ± 8.9	287.1 ± 7.7	289.5 ± 7.5	243.2 ± 7.6	252.9 ± 8.5	274.0 ± 10.7
310.0 ± 6.4	287.2 ± 5.3	290.4 ± 6.2	243.8 ± 4.7	254.5 ± 8.7	274.9 ± 15.6
311.1 ± 26.1	290.6 ± 6.4	291.8 ± 5.6	248.5 ± 9.3	263.2 ± 6.8	287.0 ± 3.6
321.6 ± 6.5	292.0 ± 8.7	308.4 ± 5.3	248.7 ± 4.9	265.1 ± 16.5	287.8 ± 12.3
326.1 ± 14.4	293.5 ± 11.2	311.6 ± 7.2	250.4 ± 7.7	271.2 ± 11.8	290.1 ± 8.0
328.5 ± 6.0	295.7 ± 10.1	312.4 ± 7.6	252.7 ± 11.4	277.0 ± 14.3	293.9 ± 4.7
329.4 ± 7.9	302.2 ± 7.1	317.2 ± 11.3	252.8 ± 9.4	280.9 ± 16.4	296.8 ± 4.8
336.0 ± 6.3	306.9 ± 10.3	339.3 ± 10.9	253.1 ± 9.6	282.5 ± 5.3	298.4 ± 3.6
341.7 ± 5.4	308.9 ± 16.3	364.7 ± 10.7	278.1 ± 6.8	283.0 ± 7.8	300.4 ± 7.7
353.9 ± 2.1	309.6 ± 10.3	364.9 ± 8.4	284.4 ± 9.2	284.0 ± 6.2	301.1 ± 7.9
354.0 ± 10.8	315.1 ± 9.1	382.4 ± 17.8	286.4 ± 7.2	284.1 ± 5.8	301.9 ± 9.1
363.6 ± 7.1	315.3 ± 16.0	409.8 ± 33.7	292.8 ± 15.6	286.2 ± 6.5	302.0 ± 5.4
380.5 ± 6.9	317.1 ± 24.7	431.6 ± 7.6	299.9 ± 8.0	287.6 ± 14.3	302.0 ± 5.1
381.1 ± 21.5	317.3 ± 23.0	442.6 ± 17.3	312.2 ± 14.4	287.9 ± 6.3	302.2 ± 8.3
381.4 ± 13.9	319.3 ± 14.8	450.2 ± 12.8	318.3 ± 11.2	292.2 ± 12.0	304.5 ± 3.2
388.2 ± 15.4	320.2 ± 13.8	450.6 ± 8.1	334.1 ± 14.0	294.8 ± 14.9	308.0 ± 3.6
412.8 ± 10.6	326.1 ± 9.1	451.9 ± 40.2	370.2 ± 13.6	297.9 ± 8.8	309.4 ± 6.8
413.7 ± 7.3	337.5 ± 12.3	453.8 ± 14.4	381.0 ± 7.3	299.2 ± 6.5	312.0 ± 7.1
414.0 ± 6.9	337.7 ± 10.6	454.9 ± 13.8	386.5 ± 17.3	300.1 ± 13.6	312.8 ± 6.0
417.5 ± 20.6	361.0 ± 5.6	455.3 ± 20.8	425.1 ± 12.1	326.6 ± 17.1	313.8 ± 11.4
425.0 ± 15.7	362.5 ± 12.5	461.0 ± 9.9	426.9 ± 11.1	332.4 ± 13.1	314.7 ± 12.3
428.8 ± 10.4	367.2 ± 13.2	463.1 ± 7.8	437.2 ± 14.3	344.6 ± 24.1	316.8 ± 6.7
430.2 ± 14.1	386.2 ± 5.2	464.0 ± 7.4	451.8 ± 29.5	347.5 ± 11.2	319.0 ± 6.7
442.1 ± 14.7	426.1 ± 20.2	464.1 ± 6.4	468.4 ± 6.5	350.9 ± 8.3	321.5 ± 7.6
442.4 ± 34.9	428.3 ± 10.5	464.1 ± 8.8	477.4 ± 19.9	353.1 ± 12.7	329.5 ± 5.1
444.8 ± 11.5	429.4 ± 11.2	465.9 ± 20.5	477.6 ± 37.3	359.9 ± 9.7	351.6 ± 9.4
445.4 ± 15.2	434.6 ± 8.7	468.2 ± 13.0	482.3 ± 27.1	364.9 ± 5.8	368.7 ± 9.9
449.9 ± 22.8	440.1 ± 5.7	470.6 ± 12.5	487.9 ± 9.4	366.7 ± 14.4	369.5 ± 14.0
451.0 ± 11.6	442.3 ± 8.7	471.4 ± 14.5	495.0 ± 12.5	375.7 ± 9.5	378.9 ± 16.1
455.0 ± 9.2	443.2 ± 14.4	472.8 ± 9.4	502.9 ± 12.2	377.1 ± 20.2	398.6 ± 15.9
456.3 ± 10.8	443.7 ± 10.8	476.3 ± 11.6	512.2 ± 19.4	380.5 ± 17.4	444.4 ± 10.6
464.3 ± 9.1	452.9 ± 25.7	479.1 ± 12.6	512.4 ± 15.5	385.3 ± 13.2	446.1 ± 19.7
464.9 ± 13.9	456.3 ± 20.2	479.6 ± 18.0	512.9 ± 21.1	388.8 ± 12.7	455.6 ± 16.6
466.8 ± 11.6	460.3 ± 12.3	485.1 ± 6.7	514.5 ± 8.9	389.8 ± 11.2	457.5 ± 8.4
468.3 ± 12.7	461.1 ± 8.4	485.9 ± 16.4	515.7 ± 20.8	396.7 ± 31.0	460.5 ± 9.3
469.4 ± 16.0	465.3 ± 10.3	487.1 ± 22.4	517.6 ± 15.6	436.3 ± 14.5	465.1 ± 11.8
470.3 ± 13.4	466.0 ± 19.1	487.4 ± 12.2	525.1 ± 15.8	437.6 ± 19.0	471.2 ± 3.3
474.1 ± 20.3	476.1 ± 9.8	487.9 ± 10.8	542.6 ± 21.5	439.4 ± 18.4	472.7 ± 16.4
474.6 ± 14.8	476.9 ± 12.5	490.4 ± 13.3	544.6 ± 15.6	446.8 ± 13.9	474.4 ± 18.3
478.7 ± 6.6	478.7 ± 21.4	490.8 ± 7.2	552.6 ± 10.1	447.6 ± 14.8	481.2 ± 15.6
478.9 ± 10.8	480.1 ± 11.1	491.1 ± 7.0	553.5 ± 17.4	451.8 ± 7.8	492.6 ± 6.1
480.5 ± 17.6	481.7 ± 11.6	513.8 ± 7.0	559.9 ± 19.5	453.4 ± 9.1	493.5 ± 14.8
481.0 ± 13.8	482.1 ± 24.1	517.2 ± 7.2	560.1 ± 14.2	456.4 ± 12.9	495.5 ± 6.3
481.7 ± 16.1	482.6 ± 13.2	518.0 ± 23.6	566.9 ± 16.5	459.9 ± 16.5	501.0 ± 7.7
483.9 ± 12.4	485.3 ± 7.4	518.2 ± 7.7	568.2 ± 35.3	465.2 ± 18.2	502.1 ± 15.1
484.1 ± 12.5	487.1 ± 16.7	518.5 ± 8.1	579.1 ± 14.6	482.9 ± 10.3	503.5 ± 11.9
484.7 ± 28.8	488.5 ± 20.2	519.8 ± 24.8	582.5 ± 19.9	500.8 ± 37.7	503.7 ± 7.6
485.5 ± 10.1	488.9 ± 14.1	526.9 ± 29.6	594.9 ± 11.8	503.7 ± 11.5	504.9 ± 19.3
487.7 ± 16.0	489.7 ± 28.8	528.5 ± 12.6	604.4 ± 28.6	507.7 ± 20.9	510.4 ± 23.8
489.1 ± 9.2	489.9 ± 14.3	528.6 ± 18.8	611.9 ± 19.5	517.6 ± 29.0	520.7 ± 17.9
492.3 ± 6.3	496.5 ± 29.8	536.1 ± 19.4	676.8 ± 17.7	539.9 ± 13.5	522.7 ± 9.3
493.6 ± 10.3	500.3 ± 17.0	549.3 ± 7.9	678.5 ± 24.9	543.3 ± 44.1	531.2 ± 25.0
496.0 ± 18.6	503.6 ± 14.6	556.6 ± 14.1	683.1 ± 13.6	565.1 ± 28.9	544.5 ± 11.9
501.8 ± 17.4	511.3 ± 22.7	567.3 ± 26.3	755.6 ± 25.1	566.9 ± 17.0	559.5 ± 23.5
508.9 ± 13.6	512.8 ± 21.4	568.4 ± 23.3	792.1 ± 15.6	569.1 ± 14.3	560.3 ± 19.5
518.4 ± 11.0	524.0 ± 12.5	585.9 ± 18.7	793.9 ± 42.7	576.5 ± 29.9	572.1 ± 17.1
518.5 ± 7.6	526.9 ± 13.6	588.4 ± 33.1	819.4 ± 24.8	600.4 ± 11.4	587.3 ± 34.9
521.5 ± 9.1	542.2 ± 9.7	594.8 ± 15.2	830.0 ± 59.2	614.6 ± 16.7	592.6 ± 10.5
525.7 ± 7.8	545.6 ± 12.2	608.0 ± 28.7	862.5 ± 24.7	615.7 ± 27.0	602.1 ± 31.9
538.6 ± 27.7	546.4 ± 19.4	611.4 ± 20.6	893.6 ± 20.3	620.5 ± 37.3	609.8 ± 13.8
541.8 ± 23.7	550.7 ± 24.8	616.7 ± 45.7	911.2 ± 30.9	685.5 ± 16.2	621.7 ± 8.0
555.6 ± 25.3	555.7 ± 24.1	623.9 ± 22.6	1061 ± 98	723.4 ± 45.2	669.1 ± 9.0
570.7 ± 36.3	576.3 ± 32.6	646.3 ± 53.1	1093 ± 104	761.4 ± 18.9	729.6 ± 15.2
578.3 ± 49.1	578.2 ± 10.0	652.6 ± 11.6	1110 ± 98	774.8 ± 31.2	741.4 ± 27.7
592.4 ± 15.9	591.3 ± 20.9	671.9 ± 26.3	1123 ± 91	867.4 ± 27.2	755.9 ± 12.9

Table 2. (continued)

Verkhoyansk			Chukotka		
00JT25	00JT26	00JT29	CH31B	CH26	CH265
594.5 ± 26.2	593.7 ± 13.8	688.9 ± 25.8	1170 ± 56	1100 ± 71	772.9 ± 16.2
601.7 ± 20.2	595.0 ± 13.6	701.3 ± 29.7	1185 ± 52	1133 ± 65	794.1 ± 13.7
652.7 ± 13.3	623.6 ± 10.9	754.0 ± 20.2	1203 ± 67	1645 ± 22	799.1 ± 22.5
689.6 ± 23.6	634.7 ± 27.0	795.7 ± 18.1	1426 ± 61	1659 ± 79	799.8 ± 27.6
826.5 ± 56.7	671.4 ± 24.4	1234 ± 90	1442 ± 58	1696 ± 77	803.6 ± 25.3
1754 ± 49	810.0 ± 16.5	1769 ± 38	1449 ± 75	1714 ± 109	810.2 ± 6.0
1800 ± 35	825.9 ± 13.0	1808 ± 18	1606 ± 47	1741 ± 109	820.2 ± 29.9
1804 ± 34	988.6 ± 18.0	1814 ± 33	1609 ± 60	1792 ± 94	836.3 ± 16.5
1839 ± 54	1801 ± 31	1814 ± 32	1610 ± 32	1798 ± 20	1017 ± 43
1862 ± 97	1832 ± 32	1825 ± 9	1626 ± 92	1808 ± 12	1039 ± 84
1864 ± 23	1845 ± 20	1827 ± 50	1634 ± 55	1822 ± 26	1050 ± 82
1888 ± 48	1888 ± 36	1918 ± 51	1638 ± 61	1835 ± 33	1051 ± 14
1922 ± 31	1911 ± 61	1921 ± 50	1645 ± 16	1835 ± 12	1067 ± 87
1948 ± 81	1931 ± 75	1980 ± 30	1649 ± 69	1844 ± 15	1097 ± 50
2028 ± 35	2014 ± 61	2313 ± 7	1655 ± 140	1856 ± 58	1120 ± 44
2069 ± 24	2021 ± 70	2379 ± 9	1662 ± 67	1876 ± 38	1210 ± 94
2073 ± 41	2044 ± 30	2384 ± 9	1691 ± 30	1945 ± 29	1273 ± 59
2501 ± 56	2445 ± 24	2431 ± 5	1758 ± 43	1983 ± 116	1755 ± 12
2543 ± 53	2446 ± 31	2432 ± 11	1785 ± 54	2005 ± 35	1826 ± 15
2581 ± 18	2447 ± 28	2495 ± 10	1842 ± 83	2028 ± 19	1829 ± 45
2668 ± 5	2479 ± 23	2506 ± 12	1847 ± 72	2143 ± 23	1831 ± 24
2728 ± 67	2500 ± 13	2570 ± 8	2334 ± 69	2215 ± 23	1842 ± 26
2788 ± 17	2537 ± 12	2596 ± 18	2430 ± 35	2266 ± 16	1862 ± 78
2829 ± 21	2730 ± 18	2605 ± 20	2821 ± 20	2468 ± 13	1950 ± 25
2986 ± 19		2612 ± 21		2478 ± 13	1955 ± 25
		2661 ± 12		3227 ± 19	1986 ± 39
		2674 ± 11			2071 ± 10
		2751 ± 10			2467 ± 11
					2591 ± 10
					2609 ± 10
					2725 ± 24

Wrangel Island	Lisburne Hills		Sadlerochit	Sverdrup	
C145741	94CL10	94CL53	96DH102	AE1	AE2
186.2 ± 4.9	223.1 ± 4.6	220.0 ± 6.7	415.9 ± 6.6	354.4 ± 10.1	376.3 ± 11.4
237.9 ± 5.7	224.7 ± 4.8	224.1 ± 6.8	420.2 ± 12.5	362.1 ± 11.8	387.9 ± 10.8
238.0 ± 9.2	226.8 ± 12.2	224.3 ± 11.5	433.1 ± 12.4	434.2 ± 4.1	426.2 ± 11.2
250.6 ± 6.3	232.2 ± 4.8	232.4 ± 13.9	445.3 ± 14.6	450.2 ± 16.5	432.4 ± 8.2
251.5 ± 15.8	232.4 ± 11.7	251.9 ± 6.4	452.7 ± 7.1	453.2 ± 7.3	447.8 ± 12.8
252.7 ± 4.6	237.4 ± 3.5	256.9 ± 5.9	453.5 ± 26.3	456.8 ± 10.5	452.6 ± 29.7
256.0 ± 20.8	240.6 ± 4.6	259.0 ± 7.2	464.7 ± 7.7	465.8 ± 14.8	464.2 ± 12.6
270.6 ± 9.1	251.5 ± 7.6	260.7 ± 9.0	466.9 ± 11.4	465.9 ± 16.2	472.1 ± 14.7
272.8 ± 23.2	252.1 ± 6.0	261.9 ± 9.7	467.4 ± 9.3	697.1 ± 58.2	473.9 ± 5.8
274.8 ± 11.5	253.1 ± 5.6	275.8 ± 4.8	469.4 ± 11.4	1045 ± 60	478.3 ± 11.7
280.1 ± 20.9	256.6 ± 4.2	306.7 ± 15.5	472.8 ± 19.9	1074 ± 88	504.2 ± 14.3
283.1 ± 9.7	258.0 ± 5.6	306.9 ± 4.4	481.9 ± 22.3	1090 ± 68	509.0 ± 7.4
285.0 ± 2.6	260.3 ± 7.8	313.9 ± 5.9	488.2 ± 15.9	1131 ± 37	509.5 ± 17.4
292.6 ± 21.3	260.4 ± 8.2	313.9 ± 12.1	512.5 ± 28.6	1135 ± 60	511.7 ± 9.0
293.6 ± 9.6	262.3 ± 6.9	314.7 ± 3.6	518.1 ± 8.9	1135 ± 30	511.7 ± 11.9
294.4 ± 9.2	267.7 ± 10.5	317.4 ± 4.8	519.0 ± 10.1	1162 ± 24	516.1 ± 18.3
298.8 ± 17.8	268.2 ± 9.4	320.8 ± 9.5	520.7 ± 13.2	1162 ± 35	530.5 ± 11.5
303.3 ± 11.2	269.3 ± 8.7	321.5 ± 11.2	520.8 ± 11.9	1187 ± 56	531.4 ± 8.6
317.3 ± 18.9	270.1 ± 7.6	323.3 ± 11.1	520.9 ± 19.8	1204 ± 47	534.7 ± 9.6
323.9 ± 11.3	272.7 ± 8.8	325.8 ± 19.8	522.6 ± 23.2	1207 ± 25	536.3 ± 13.1
361.7 ± 5.8	273.1 ± 8.2	327.2 ± 14.3	523.0 ± 11.4	1208 ± 32	536.5 ± 8.8
375.2 ± 14.6	276.8 ± 4.7	327.9 ± 12.0	524.7 ± 10.8	1212 ± 79	540.0 ± 9.6
395.7 ± 7.1	277.3 ± 3.7	328.6 ± 8.6	524.9 ± 21.7	1216 ± 13	543.7 ± 9.7
397.8 ± 13.7	317.9 ± 8.0	339.8 ± 7.4	526.3 ± 10.6	1228 ± 62	548.0 ± 10.6
424.7 ± 14.1	320.4 ± 9.9	347.6 ± 10.5	526.7 ± 15.3	1228 ± 31	549.8 ± 26.3
435.5 ± 11.0	321.2 ± 14.3	356.9 ± 8.3	528.4 ± 16.1	1233 ± 82	549.9 ± 22.6
440.7 ± 14.4	323.9 ± 11.9	359.6 ± 8.5	528.9 ± 8.5	1234 ± 93	550.3 ± 20.2
443.3 ± 15.8	324.2 ± 10.5	359.7 ± 16.9	529.4 ± 13.8	1250 ± 91	551.3 ± 13.3
448.0 ± 11.8	325.8 ± 8.2	360.3 ± 9.3	531.3 ± 17.3	1265 ± 45	551.9 ± 26.2
454.6 ± 6.2	327.4 ± 23.8	361.3 ± 16.8	532.5 ± 12.7	1271 ± 24	552.8 ± 13.5
461.2 ± 21.0	330.7 ± 9.4	365.9 ± 13.8	533.6 ± 5.2	1290 ± 59	554.3 ± 20.4
510.7 ± 15.7	332.0 ± 12.6	368.0 ± 10.9	534.5 ± 17.6	1306 ± 21	554.7 ± 10.5

Table 2. (continued)

Wrangel Island	Lisburne Hills		Sadlerochit	Sverdrup	
C145741	94CL10	94CL53	96DH102	AE1	AE2
667.6 ± 17.7	334.3 ± 11.4	369.0 ± 14.3	539.7 ± 9.4	1374 ± 30	556.4 ± 24.9
751.5 ± 30.6	336.5 ± 16.3	381.4 ± 8.6	549.4 ± 17.3	1376 ± 43	558.3 ± 12.3
1059 ± 83	359.3 ± 14.4	416.3 ± 19.7	550.0 ± 9.3	1396 ± 43	559.6 ± 13.3
1084 ± 55	359.8 ± 11.3	421.9 ± 11.6	553.6 ± 38.9	1609 ± 96	559.7 ± 11.7
1110 ± 47	363.4 ± 11.6	422.8 ± 18.0	554.3 ± 14.7	1610 ± 38	561.3 ± 17.5
1188 ± 106	365.0 ± 17.0	423.4 ± 9.4	557.1 ± 21.9	1641 ± 24	562.2 ± 12.0
1613 ± 61	366.1 ± 19.6	429.0 ± 12.6	558.8 ± 12.2	1643 ± 17	563.1 ± 32.5
1699 ± 20	369.2 ± 8.5	430.4 ± 19.0	560.8 ± 17.5	1646 ± 37	566.5 ± 11.5
1717 ± 10	373.7 ± 12.6	431.1 ± 16.4	560.8 ± 26.9	1653 ± 52	567.1 ± 27.4
1832 ± 33	374.3 ± 8.5	431.7 ± 18.1	563.6 ± 9.1	1666 ± 28	567.1 ± 11.2
1892 ± 19	375.5 ± 11.8	433.5 ± 35.7	564.1 ± 10.0	1666 ± 49	567.6 ± 21.7
1926 ± 22	406.4 ± 6.8	434.1 ± 12.8	564.3 ± 23.8	1667 ± 19	567.6 ± 18.6
1947 ± 26	419.1 ± 6.1	436.0 ± 19.1	564.7 ± 9.6	1673 ± 25	569.2 ± 16.1
1977 ± 18	423.0 ± 14.8	439.2 ± 10.7	566.5 ± 17.2	1696 ± 19	569.4 ± 26.1
2129 ± 19	423.9 ± 14.9	440.7 ± 14.5	568.0 ± 15.6	1708 ± 17	570.9 ± 6.0
2384 ± 15	425.1 ± 12.7	443.6 ± 10.8	570.0 ± 10.3	1711 ± 31	572.2 ± 10.5
2435 ± 9	428.8 ± 10.1	449.6 ± 19.6	572.2 ± 20.4	1723 ± 21	572.2 ± 12.4
2454 ± 19	429.4 ± 12.7	452.4 ± 17.1	573.2 ± 8.7	1730 ± 27	572.2 ± 17.2
2492 ± 20	429.6 ± 12.3	453.0 ± 17.4	577.3 ± 24.0	1742 ± 18	572.5 ± 16.7
	431.6 ± 8.0	453.7 ± 11.5	579.2 ± 14.3	1744 ± 20	574.6 ± 17.2
	438.7 ± 12.9	481.5 ± 17.2	582.7 ± 18.2	1751 ± 43	574.7 ± 15.4
	439.9 ± 16.8	536.6 ± 19.0	585.8 ± 22.0	1754 ± 35	575.3 ± 16.7
	440.0 ± 11.7	537.9 ± 19.4	589.8 ± 24.7	1763 ± 22	578.4 ± 12.9
	440.3 ± 12.0	544.2 ± 14.7	590.3 ± 24.3	1764 ± 34	578.4 ± 14.7
	442.3 ± 8.0	561.3 ± 19.4	595.2 ± 12.5	1775 ± 18	578.5 ± 10.0
	445.6 ± 13.4	569.0 ± 33.6	599.3 ± 15.7	1776 ± 21	585.8 ± 16.2
	450.7 ± 23.7	598.4 ± 7.8	614.2 ± 28.0	1779 ± 29	587.1 ± 16.1
	450.9 ± 30.5	611.1 ± 21.1	615.7 ± 7.7	1786 ± 21	587.5 ± 17.8
	452.3 ± 12.5	611.2 ± 20.0	616.7 ± 20.5	1799 ± 19	589.6 ± 20.6
	456.3 ± 9.2	677.6 ± 7.7	623.5 ± 30.0	1803 ± 17	590.7 ± 20.2
	459.6 ± 17.5	799.4 ± 21.5	679.1 ± 21.0	1841 ± 52	600.3 ± 20.4
	490.5 ± 10.4	817.4 ± 13.6	681.1 ± 10.1	1847 ± 21	607.4 ± 25.3
	518.0 ± 11.6	867.2 ± 14.3	684.8 ± 27.1	1870 ± 24	608.3 ± 20.8
	553.5 ± 11.7	870.7 ± 23.2	874.1 ± 12.2	1904 ± 84	619.5 ± 12.7
	581.9 ± 23.7	904.5 ± 20.6	882.1 ± 20.4	1919 ± 25	621.4 ± 32.4
	600.5 ± 9.7	908.3 ± 26.8	883.4 ± 10.2	1932 ± 28	629.5 ± 38.7
	615.1 ± 17.9	974.5 ± 34.0	893.9 ± 23.2	1933 ± 20	662.1 ± 12.9
	638.5 ± 16.6	1066 ± 84	895.8 ± 31.5	1937 ± 19	663.0 ± 17.9
	644.6 ± 23.7	1204 ± 66	916.1 ± 30.6	1945 ± 23	675.1 ± 24.0
	646.7 ± 16.1	1227 ± 69	950.3 ± 39.9	1986 ± 13	751.1 ± 15.9
	662.3 ± 25.8	1243 ± 62	1049 ± 22	1993 ± 17	906.3 ± 39.3
	739.0 ± 40.0	1277 ± 50	1058 ± 37	2020 ± 19	921.2 ± 9.0
	751.7 ± 30.7	1362 ± 69	1065 ± 11	2024 ± 19	1021 ± 65
	805.3 ± 28.9	1454 ± 55	1069 ± 22	2397 ± 33	1058 ± 28
	815.8 ± 46.8	1499 ± 71	1095 ± 77	2432 ± 18	1076 ± 83
	909.1 ± 23.0	1846 ± 48	1097 ± 73	2476 ± 26	1115 ± 56
	928.4 ± 20.6	1862 ± 46	1140 ± 50	2488 ± 40	1129 ± 28
	1228 ± 66	1903 ± 11	1160 ± 38	2599 ± 16	1170 ± 51
	1292 ± 57	1955 ± 49	1195 ± 62	2695 ± 17	1210 ± 82
	1715 ± 47	1963 ± 42	1204 ± 48	2724 ± 16	1211 ± 43
	1722 ± 66	1977 ± 26	1218 ± 54	2736 ± 17	1257 ± 42
	1747 ± 18	1986 ± 39	1228 ± 45	2834 ± 18	1265 ± 50
	1767 ± 89	2033 ± 12	1239 ± 57	2938 ± 16	1277 ± 34
	1834 ± 36	2149 ± 25	1607 ± 19	3184 ± 16	1354 ± 75
	1876 ± 31	2274 ± 21	1654 ± 36		1473 ± 20
	1953 ± 41	2329 ± 47	1765 ± 41		1610 ± 68
	2051 ± 23	2352 ± 17	1849 ± 9		1612 ± 33
	2063 ± 71	2490 ± 15	1970 ± 21		1657 ± 18
	2136 ± 32	2512 ± 7	1985 ± 47		1693 ± 44
	2166 ± 16	2536 ± 37	2609 ± 21		1832 ± 17
	2302 ± 18	2555 ± 24	2636 ± 15		1833 ± 17
	2674 ± 12		2638 ± 28		1845 ± 47
			2681 ± 33		1858 ± 25
					1883 ± 37

[a]Ages are in Ma. Uncertainties are at the 95% confidence interval. Interpreted ages for grains <1.2 Ga are $^{206}Pb/^{238}U$ ages. Interpreted ages for grains >1.2 Ga are $^{206}Pb/^{207}Pb$ ages. The complete isotopic and age data can be found in Table S1.

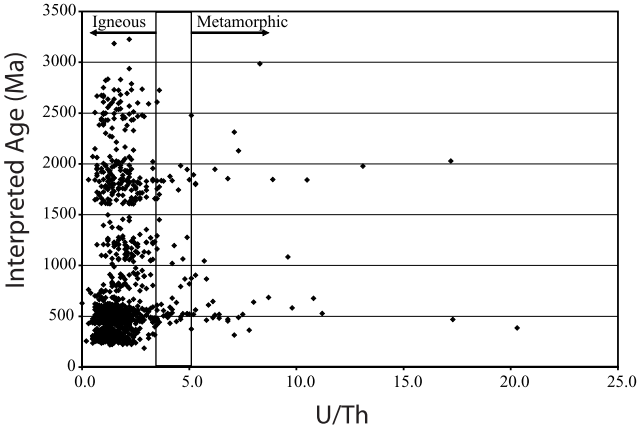

Figure 4. U/Th of spot analyses of zircons from circum-Arctic Triassic strata. U/Th is determined on the same material analyzed for U-Pb age and is calibrated relative to NBS SRM 610 trace element glass. Zircon that has U/Th of less than 3 is igneous in origin, whereas zircon with U/Th greater than 5 probably grew during regional metamorphism [*Williams*, 2001; *Rubatto et al.*, 2001].

The Middle Triassic Tolbon Formation consists of mostly nonmarine, plant fossil bearing sandstone and siltstone with some intraformational conglomerate. On the basis of thin section analyses, sandstones consist of quartz (35–65%), feldspar (5–30%), rock fragments (25–45%) and matrix (5–10%). Rock fragments include granodiorite, volcanic rocks and chert. The upper Tolbon Formation has a greater percentage of sandstone and is characterized by the appearance of pebbles of quartz, chert, igneous and metamorphic rocks. Heavy mineral suites include garnet and mica [*Kossovskaya et al.*, 1960]. Post-1200 Ma peaks in the detrital zircon age probability distribution of Middle Triassic sample JT-25 include those of age 331, 353, 381, 422, and 477 Ma, represented by zircon age ranges of 320–345, 350–365, 375–395, 410–435, and 440–495 Ma (Table 3 and Figure 5).

[21] The Upper Triassic Khadalichen Formation consists of sandstone, siltstone, grit and gravel. Sandstones are quartz-rich and consist of quartz (50–95%), feldspar (5–25%), and rock fragments (5–25%). Pebbles include granite porphyry, tuffs, quartz, chert, sandstone and siltstone, granodiorite and other igneous and metamorphic rocks. Heavy minerals include leucoxene, mica and zircon [*Kossovskaya et al.*, 1960]. The detrital zircon populations from the two upper Triassic sandstones dated are similar. Sample JT26 includes peaks of 292, 321, 439 and 483 Ma represented by zircon age ranges of 275–300, 300–330, 425–455, and 455–505 Ma (Table 3 and Figure 5). Sample JT29 includes peaks of 292, 308, 459, 485 and 517 Ma represented by zircon age ranges of 265–300, 300–320, 450–475, 475–495, and 510–530 Ma (Table 3).

[22] The abundance of Paleozoic ages (as compared to Precambrian ages) in these three samples (Table 3 and Figure 6) are compatible with an inferred source for Triassic sediments of the Verkhoyansk margin in the Baikal Mountain region along the southern margin of the North Asia craton, known to have been an active, Andean-style margin throughout the late Paleozoic [e.g., *Sengor and Natalin*, 2004]. Notably, the Angara-Vitim batholith of the central Baikal Mountains extends over 800 km along strike and has a width of over 300 km. K-Ar, Rb-Sr, and U-Pb methods suggest formation of the batholith in the Late Caboniferous–Early Permian during the approximate time interval 290–320 Ma [e.g., *Bukharov et al.*, 1992; *Yarmolyuk et al.*, 1997; *Wickham et al.*, 1995]. This age range corresponds nicely with the youngest detrital zircon age peaks in Late Triassic sandstone samples of the Verkhoyansk (peaks at 292, 292,308 and 321). Zircon ages in Middle Triassic sample JT25 overlap with this age range, but are somewhat older with peaks at 331, 353 and 381. Ordovician and Cambrian volcanic and plutonic arc rocks are also present in the accretionary collage of the Baikal Mountains but are not as well dated. It is likely, however, that these units were actively eroding by the Permo-Carboniferous [*Sengor and Natalin*, 2004] and thus could have supplied the older, mostly Siluro-Ordovician-Cambrian zircons present in Triassic sandstone samples from the northern Verkhoyansk.

4.2. Chukotka and Wrangel Island (Locations 2 and 3)

[23] The Triassic of Chukotka is represented by up to 5.5 km of mostly distal turbidite sequences that range upward into shelf deposits of Upper Triassic (Norian) age [*Bychkov*, 1994]. They are almost everywhere tightly folded and variably metamorphosed and their stratigraphy and sedimentology have not been studied in detail. Triassic basinal sequences were deposited above Carboniferous and Permian carbonate platform sequences across both Chukotka and Wrangel Island [e.g., *Belik and Sosunov*, 1969; *Polae*, 1966; *P'yankov*, 1981; *P'yankov and Huppenen*, 1974; *Zheltovski*, 1976; *Zhuravlev*, 1976; *Kos'ko et al.*, 1993]. Lower Triassic strata are intruded by gabbroic sills and dikes that have yielded conventional K-Ar whole rock ages ranging from 250 to 190 Ma but have not been dated by more precise methods [*Bychkov and Gorodinsky*, 1992; *Gelman*, 1963; *Ivanov and Milov*, 1975]. Triassic sandstones are mostly fine grained with compositions varying from ''continental block'' to ''recycled orogen'' [*Tuchkova et al.*, 2004]. Multiple source areas are represented: sandstones are either characterized by an abundance of intermediate to mafic volcanic lithic fragments or by quartz, feldspar and metamorphic lithic fragments [*Tuchkova et al.*, 2004]. We analyzed two Middle Triassic (Carnian) samples and one Upper Triassic (Norian) sample. Zircon populations from these three samples are quite similar (Figure 5). The two Carnian samples (CH2.6 and CH3.1B) are the most similar. Sample CH2.6 has zircon age peaks at 249, 288, 361, 452 and 565 Ma, represented by grain age ranges of 240–255, 275–305, 340–390, 435–470, and 560–580 Ma (Figure 5 and Table 3). Sample CH3.1B has zircon age peaks at 244, 285, 381, 430, 475, 512 and 555 Ma, represented by grain age ranges of 235–255, 275–300, 370–390, 495–530, and 540–585 Ma (Figure 5 and Table 3). Upper Triassic (Norian) sandstone sample CH26.5 includes

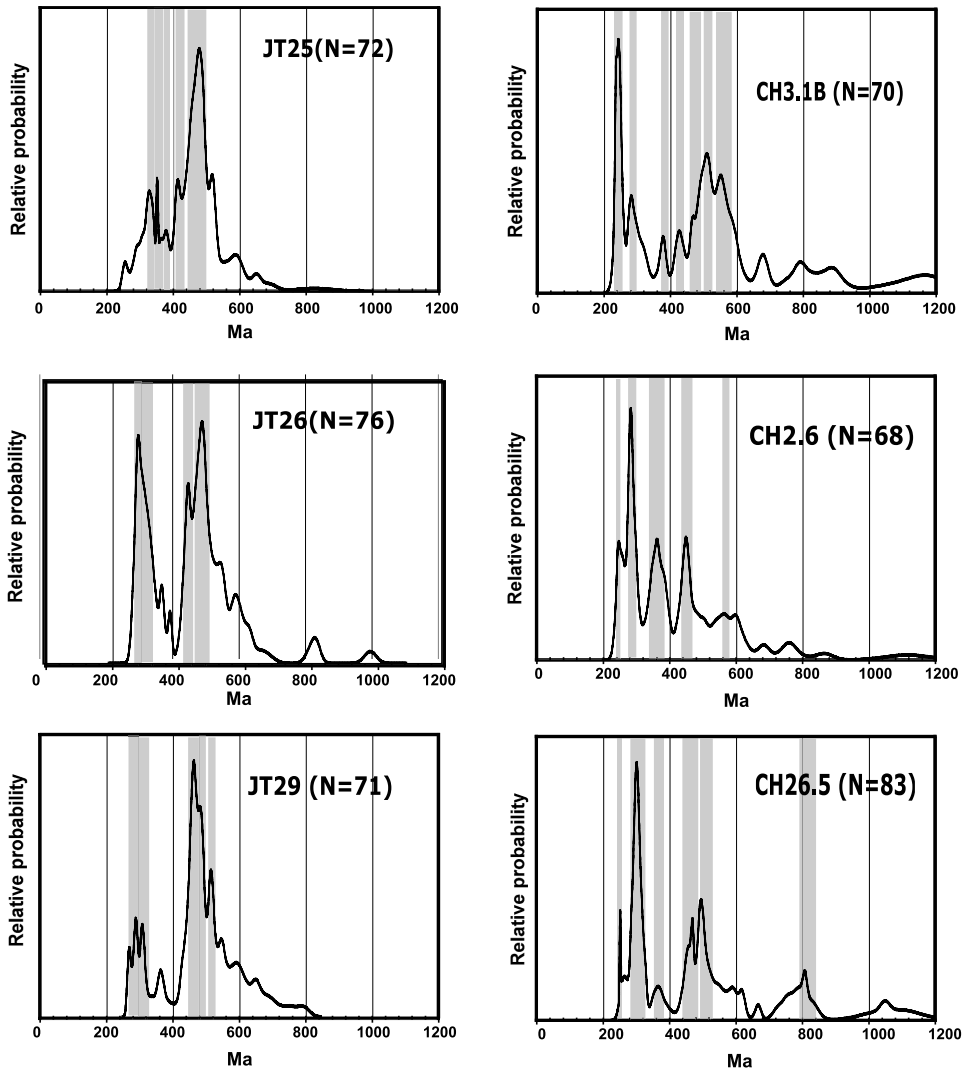

Figure 5. Relative probability distribution diagram for detrital zircon U-Pb ages from Triassic sandstones from the northern Verkhoyansk (JT25, 26 and 29) and Chukotka (CH3.1B, CH2.6 and CH26.5). Sample localities are listed in Table 1 and shown on Figure 1. Height of peak is proportional to the probability that these ages are present in the sample, with the area under the curve equal to 1. Only grains with ages 0–1200 Ma are displayed; all data from combined samples are shown in Figure 6. Grey bars represent the range of grain ages of selected age peaks listed in Table 3. See Table 3 for selection criteria.

age peaks of 253, 304, 367, 467, 498 and 811 Ma, represented by grain age ranges of 250–265, 285–330, 350–380, 440–485, 490–525, and 790–840 Ma (Figure 5 and Table 3). With the exception of the 555 and 565 age peaks in samples CH2.6 and CH3.1B, the range of ages represented by peaks in all three of these samples overlap (Figure 5).

[24] The Triassic detrital data of Chukotka is distinguished from that of the Verkhoyansk by its inclusion of an important component of Permo-Triassic zircons. Permo-Triassic age peaks in these three samples at 244, 249 and 253 Ma, representing a single-grain age range of 235 to 265 Ma (Figure 5), lie within error of Siberian Trap magmatism (248–253 Ma) [e.g., *Campbell et al.*, 1992; *Venkatesan et al.*, 1997; *Renne and Basu*, 1996]. Siberian Trap magmatism was dominantly basaltic, thus might have only contributed partially to the zircon populations of Triassic sandstones in Chukotka. Associated silicic intrusions and tuffs may be occasionally present in the vicinity of the Siberian Traps but are not widely described. If these were more widespread at the time, it is possible that the Siberian Traps could be one of the sources of the Triassic of Chukotka. Alternatively, in the Taimyr Peninsula there are scattered 241–249 Ma high-level syenitic to granitic stocks that have been linked to the mantle plume that generated the Siberian Traps [*Vernikovsky et al.*, 2003]. Their erosion could have also provided the Permo-Triassic zircons seen in Chukotka samples. Tuffs and tuffaceous sediments have been described in the Late Permian and earliest Triassic deposits of Chukotka [*Chasovitin and Shpetnyi*, 1964; *Belik and Sosunov*, 1969;

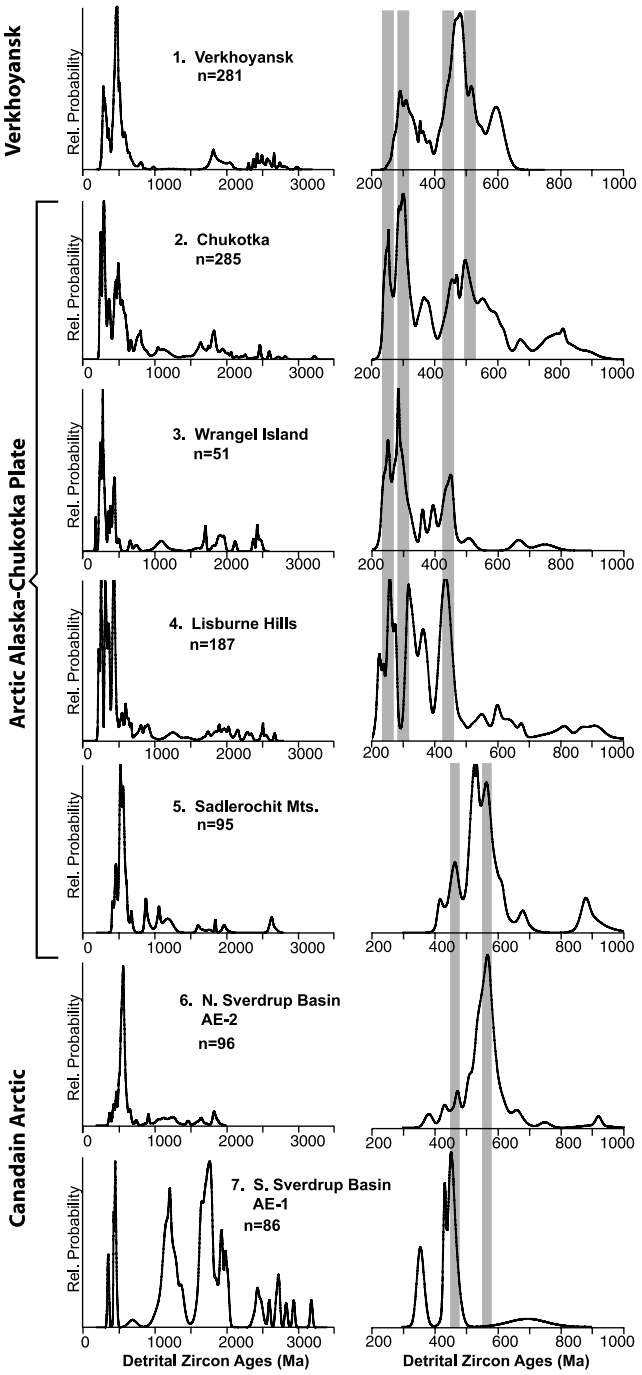

Figure 6. Relative probability distribution diagrams for detrital zircon U-Pb ages from Triassic sandstones in the Arctic. Sample locations shown in Figure 1. Height of peak is proportional to the probability that these ages are present in the sample, with the area under the curve equal to 1. On the left, spectra include all of the ages from each sample. On the right, spectra include only ages <1000 Ma.

Sosunov and Til'man, 1960] but have never been dated radiometrically. These could represent an even more local origin for zircons in overlying Triassic deposits. If the Triassic of Chukotka was derived from the Taimyr region or more locally, it is surprising how many of the age peaks in Chukotka correspond with those of the Verkhoyansk. In particular, the three samples from Chukotka contain Late Carboniferous–Early Permian age peaks at 285, 288 and 304 Ma, similar to age peaks in the Verkhoyansk samples (292, 292 and 308). However, these detrital ages also match the known ages of widespread, voluminous and well dated collisional to postcollisional granitoids of the northern Taimyr Peninsula (with reported ages ranging from 264–300 Ma [*Vernikovsky*, 1996]) and Permian granitoids in the Urals east of the Trans-Uralian fault [*Scarrow et al.*, 2002; *Bea et al.*, 2002]. The Devonian age peaks present in Chukotka samples (361, 367 and 381) are similar in age as those reported from Middle Triassic sample JT25 from the Verkhoyansk (331, 353 and 381Ma) (Table 3) but plutons of this age (340–390 Ma) are known to also be present in the Arctic Alaska-Chukotka microplate itself and in the Urals [*Scarrow et al.*, 2002]. Ordovician zircon age peaks from Chukotka (409, 430, 450, 475 and 498 Ma) are also similar to those of the Verkhoyansk samples (422, 439, 459, 477, 483, 485 Ma). Cambrian and late Precambrian peaks are more common in Chukotka samples (512, 555, 565, 811, and 720–920 Ma) than in Verkhoyansk samples (JT29 has a 517 Ma peak). These peak ages from Chukokta are not unlike the age range of scattered plutons dated in the Precambrian basement of Arctic Alaska-Chukotka (a known spread from 550–750 Ma). No U-Pb ages in the 460–630 Ma range are reported from the Urals [*Scarrow et al.*, 2002], but 566 to 800 Ma U-Pb zircon ages from calc-alkaline granites and plagiogranites are known in the Taimyr Peninsula [*Vernikovsky*, 1996]. Finally, Triassic sandstones from Chukotka contain zircons with a range of ages from 750 to 1000 Ma and zircons ranging from 1000 to 1300 Ma are common. These ages are not present in the Verkhoyansk samples (Figure 5 and Table 3). In the Taimyr, granitoids with U-Pb zircon ages ranging from 840 to 1004 Ma are reported [*Pease et al.*, 2001; *Pease and Vernikovsky*, 2000; *Vernikovsky et al.*, 1988].

[25] Triassic strata of Wrangel Island consist of a 0.8 to 1.5 km thick succession of dark, unfossiliferous, interstratified sandstones, siltstones and shales deposited in a basinal setting [*Kos'ko et al.*, 1993]. Like Chukotka, the Triassic strata of Wrangel Island are inferred to have been deposited across Permian carbonate platform deposits. Unlike Chukotka, there are no mafic dikes and sills. The sandstones consist predominantly of quartz. A single small sample of Triassic sandstone from Wrangel Island yielded 51 datable zircons (Figure 6 and Tables 2 and 3). Phanerozoic zircon age peaks occur at 252, 283, and 450 Ma, representing age ranges of 235–260, 270–305, and 435–465 Ma. Grains with ages in the 1000–1300 Ma interval are also present. These age peaks are indistinguishable from the zircon ages in Chukotka samples. This is expected because Wrangel Island is geographically, stratigraphically and structurally linked to mainland Chukotka. It is separated from the mainland by a younger sedimentary basin, the along-strike continuation of the Tertiary Hope Basin of the Bering Shelf [*Tolson*, 1987] (Figure 3). Although the data set from Wrangel Island is not as robust as that describing the Triassic of Chukotka, the similarity in detrital zircon ages

Table 3. Interpreted Peak Ages and Age Ranges

Peak Age,[a] Ma	Number of Grains[b]	Age Range,[c] Ma
	JT25 (N = 93)	
331	6	320–345
353	3	350–365
381	4	375–395
422	9	410–435
477	28	440–495
	9	1740–1960
	3	2020–2080
	8	2500–3000
	JT26 (N = 92)	
292	9	275–300
321	11	300–330
439[c]	9	425–455
483[c]	21	455–505
	6	1800–1940
	3	2000–2060
	6	2440–2540
	JT29 (N = 96)	
292	6	265–300
308	4	300–320
459[c]	15	450–475
485[c]	11	475–495
517	9	510–530
	6	1760–1840
	14	2300–2760
	94CL10 (N = 94)	
232[c]	7	220–245
265[c]	17	250–280
326	11	315–340
369	9	355–380
436	19	415–460
	6	600–665
	10	1700–2180
	94CL53 (N = 93)	
223	4	220–265
256	5	250–265
321	13	305–330
360	7	355–370
436	18	415–455
	8	530–620
	7	1840–2040
	4	2480–2560
	4	1200–1280
	96DH102 (N = 95)	
467	10	445–490
530	20	510–540
565	22	545–590
	7	860–960
	13	1040–1240
	4	2600–2700
	AE1 (N = 86)	
454	6	430–470
1216	15	1130–1240
1662	8	1640–1675
1769	13	1730–1805
1933	5	1920–1950
1988	4	1985–2025
	10	2380–2940
	AE2 (N = 96)	
474	4	460–480
511[c]	6	500–520
566[c]	45	530–590
	11	1020–1280
	4	1600–1700
	5	1820–1900
	CH13B (N = 92)	
244	11	235–255
285	5	275–300
381	3	370–390
430	3	425–440
475	5	465–490
512	9	495–530
555	10	540–585
	8	725–920
	7	1060–1220
	15	1600–1860
	CH26 (N = 94)	
249	5	240–255
288	14	275–305
361	13	340–390
452	10	435–470
565	4	560–580
	14	1640–1880
	CH26.5 (N = 99)	
253	3	250–265
304	23	285–330
367	4	350–380
467	10	440–485
498	11	490–525
811	7	790–840
	8	1000–1280
	10	1740–2080
	C145741 (N = 51)	
252	6	235–260
283	11	270–305
450	6	435–465
	4	1040–1200
	8	1600–1980
	4	2380–2500

[a]Most peak ages listed above are prominent peaks on relative age-probability diagrams (Figures 5 and 6). Peak ages are reported only for age ranges that define a single obvious peak. The listed peaks include at least three overlapping analyses (within about a million years of each other and with low reported errors). Peak age determined by deconvolution of adjacent peaks using the Sambridge-Compston algorithm in Isoplot 3.0 [*Ludwig*, 2003].

[b]Number of grains is the number of grains included in an age range.

[c]Age range is the range of ages that make up a cluster on a relative age-probability diagram (Figures 5 and 6).

would argue that sequences of both regions formed part of a once continuous depositional system or basin in the Triassic.

4.3. Lisburne Hills (Locality 4)

[26] The Lisburne Hills fold-and-thrust belt in westernmost Alaska (Figure 3) consists of lower Paleozoic to Mesozoic sedimentary rocks involved in Brookian thrusting [*Moore et al.*, 2002]. Two samples were collected from an unusual sandstone member of the Triassic Otuk Formation. The sandstone lies stratigraphically between the shale and chert members of the Otuk as described by *Blome et al.*

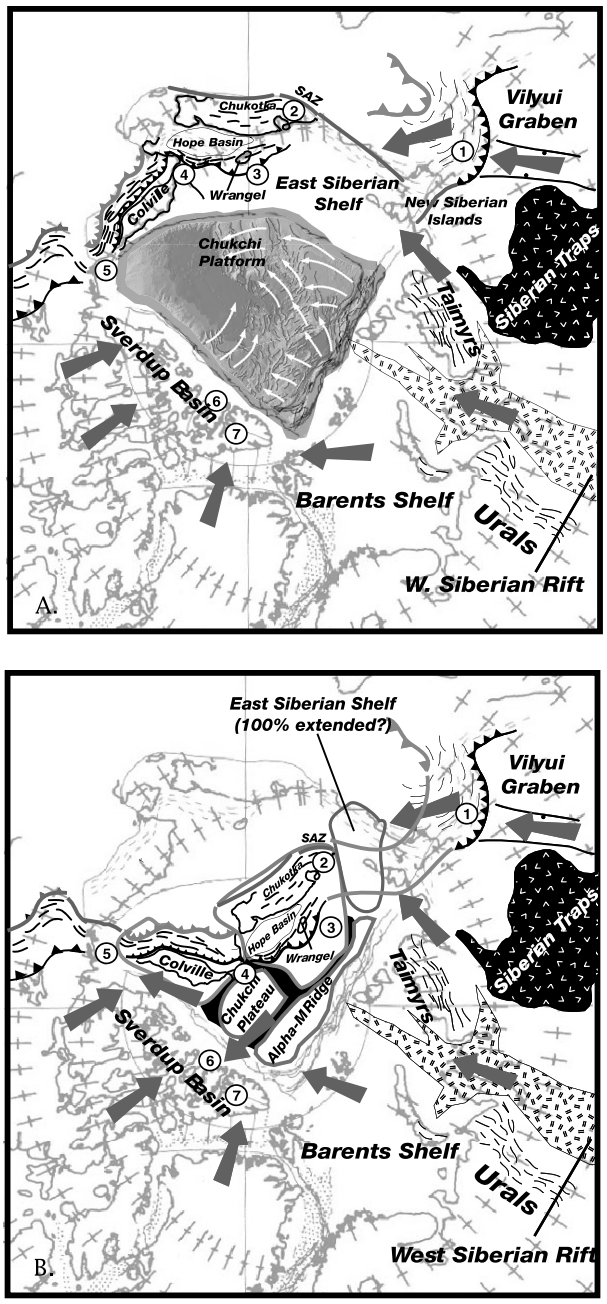

Figure 7. Speculative reconstruction of the Amerasian Basin that accounts for U-Pb single-grain detrital ages in Triassic sediments. Base map is from *Rowley and Lottes* [1988] and shows the plate reconstruction for the Arctic prior to the opening of the North Atlantic. The Lomonosov Ridge has been restored against the Barents Shelf, and the Amerasian Basin is assumed to be as it now exists. The reconstruction represents the end of the Jurassic and beginning of the Cretaceous, prior to opening of the Amerasian Basin, but does not restore shortening-related deformation that took place at this time. Grey arrows show inferred sediment source directions in the Triassic. The polar Urals may have acted as a divide in the Triassic with respect to river systems and sediment transport. For further discussion, see text.

[1988] and is very fine to fine-grained, massive, and about 5 m thick. *Monotis* fossils found in the sandstone suggest a Late Triassic age. The sandstone is lithic, consisting of about 40% monocrystalline quartz, 20% altered feldspar, and 40% lithic fragments (argillite, chert, siltstone, granitic fragments and carbonate). The Otuk in general is thought to represent condensed sedimentation in an outer shelf environment [*Moore et al.*, 1994]. Although a predominantly sedimentary provenance is inferred for this sandstone, the granitic fragments suggest that it was shed from a source region that lay to the NW (present coordinates) in the offshore Chukchi platform region (K.W. Sherwood, written communication, 2000, as cited by *Moore et al.* [1994]). The two samples from the Lisburne Hills, 94CL10 and 94CL53, have very similar zircon age populations. Individual peaks and the age ranges represented are listed in Table 3; age probability plots are combined in Figure 6. The samples include Triassic peaks that are younger than any peaks present in previously discussed samples. Age peaks of 232 and 223 Ma, characterized by grain age ranges of 220–245 and 220–265 Ma overlap the grain age ranges that define Permo-Triassic age peaks in samples from Chukotka and Wrangel Island, but include some younger single-grain ages (Tables 2 and 3). Peak ages of 256 Ma, in both samples dated, correspond to age ranges of 250–280 and 250–265 Ma and also overlap the single-grain age ranges represented by Permo-Triassic age peaks of Chukotka and Wrangel Island samples, but include some older single-grain ages. When the data from the two Lisburne Hills samples are grouped (Figure 6), with a total of 187 single-grain ages represented, two distinct age peaks are further resolved, one at 222 Ma and the other at 255 Ma. Thus it appears that the Lisburne samples contain a Permo-Triassic zircon population as does Chukotka, but might also contain a distinctly younger population of zircons that are about 222 Ma old (Late Triassic). Carboniferous age peaks at 321 and 326 Ma, represented by single-grain age ranges of 305–330 and 315–340 Ma are similar, but slightly older than age peaks in samples from Chukotka (288 and 304 Ma represented by age ranges of 275–305 and 285–330 Ma). Age peaks of 360 and 369 Ma in the Lisburne samples, represented by age ranges of 355–370 and 355–380 Ma, are similar to those in Chukotka samples (361, 367 and 381 Ma, represented by age ranges of 340–390, 350–380, and 370–390 Ma) and again, are known to correspond to the range of U-Pb ages obtained from Devonian plutons in northern Alaska and Chukotka (340–390 Ma). Well-defined age peaks in each of the Lisburne samples at 436 Ma, representing an age span of 415–460 Ma (at least 37 single-grain ages represented) are identical to important age peaks seen in Chukotka and Verkhoyansk samples. Finally, both samples from the Lisburne Hills have zircons that span 530–665 Ma. These ages are present in samples from Chukotka, but are not present in all Verkhoyansk samples (Late Triassic sample JT29 has a 517 Ma peak represented by grains 510–530 Ma). In summary, Triassic sandstone of western Alaska, although deposited in a very different setting than sandstones of Chukotka and Wrangel Island (shelf facies sandstone versus basinal turbidites) shared similar source regions for their detrital

zircons populations. Samples from westernmost Alaska differ in their inclusion of a younger Triassic zircon population of about 222 Ma. The closeness in age of this peak to the depositional age of the sandstone might suggest derivation from a contemporaneous magmatic source.

4.4. Sadlerochit Mountains, Eastern Alaska (Locality 5)

[27] Detrital zircons from a single sample from the Early Triassic Ledge Member of the Ivishak Formation of the Sadlerochit Mountains in northeastern Alaska were dated (Figures 1 and 3). Sedimentary structures and burrows indicate a shallow marine deltaic origin for the Ledge Member, which, based on sedimentary facies and paleocurrent directions, is known to have been derived from the north (present-day coordinates) [*Mariani*, 1987]. This unit is also notable because it is the main oil reservoir of the Prudhoe Bay field. The detrital zircon ages from the Ledge Member of the Ivishak Sandstone are strikingly different from those of the Triassic of the Lisburne Hills, discussed above. The sample from the Sadlerochit Mountains exhibits age peaks at 467, 530 and 565 Ma, represented by age ranges 445–490, 510–540, and 545–590. Permo-Triassic, Permo-Carbonifereous, and Devonian age peaks are conspicuously absent (Table 3 and Figure 6). The youngest age peak, 467 Ma, falls within the range of the prominent Ordovician peaks seen in all of the samples discussed so far. Cambrian to Late Precambrian zircons form an important component of the detrital population of this sample, with peaks at 530 and 565 Ma representing age spans of 510–540 Ma (20 grains) and 545–590 Ma (22 grains). These ages correspond to the youngest age limit of late Precambrian plutons that have been dated in basement rocks of northern Alaska and Wrangel Island [*Moore et al.*, 1994; *Amato et al.*, 2003; *Amato*, 2004; *Kos'ko et al.*, 1993]. It seems that rocks of this age, or sediments derived from them must have been quite prevalent in the northern source area for these sandstones.

4.5. Sverdrup Basin, Arctic Canada (Locations 6 and 7)

[28] Sample AE-2 is representative of the Late Triassic (upper Carnian) sandstone-dominated Pat Bay Formation, a fine-grained, shallow marine shelf-facies sandstone. The Pat Bay Formation exhibits facies changes (shallower water to the north) that argue that the main region of sediment supply for the northern Sverdrup Basin in the Late Triassic lay to the present north of the basin [*Embry*, 1991, 1992]. Not much is known about this northern landmass because rifting associated with formation of the Amerasian Basin has removed the northern margin of the Sverdrup Basin, which now lies foundered beneath the continental shelf and slope of the Canadian Arctic margin [*Embry*, 1992]. This paleosource region was termed "Crockerland" by *Embry* [1992] and it provided sediments to the Sverdrup Basin intermittently from the Carboniferous to the Jurassic [*Embry*, 1992]. The detrital zircon population from the Pat Bay Formation helps characterize "Crockerland". The younger age peaks in this sample are virtually identical to those of the Ledge Sandstone Member of the Ivashak Formation of easternmost Alaska. Peaks are evident at 474, 511 and 566 Ma, represented by grain age ranges of 460–480, 500–520, and 530–590 Ma. As in the Sadlerochit Mountains, the 566 Ma age peak, represented by 45 grains out of a total of 96 grains is conspicuous. In addition, significant numbers of single-grain ages fall in the intervals 1020–1280, 1600–1700, and 1820–1900. The similarities between the zircon populations from the Triassic of the Sadlerochit Mountains and Triassic sediments derived from the northern borderland of the Sverdrup Basin suggest that the now missing "Crockerland" might well have sourced both these regions.

[29] Sample AE-1 (location 7, Figure 1) is representative of the Early Triassic (Smithian) braided stream facies of the Bjorne Formation from central Ellesmere Island. On the basis of facies changes from fluvial-deltaic sands to the SE, to nearshore, offshore shelf, and basinal shales and siltstones to the NW, the Bjorne Formation is believed to have been sourced from the east and south of the region sampled [*Embry*, 1991]. The deltaic sediments were fed by major river systems flowing from the Greenland and Canadian Shield regions [*Embry*, 1991]. A 454 Ma Ordovician age peak is evident in the zircon population of the Bjorne Formation (Table 3 and Figure 6), represented by six grains with ages ranging from 430 to 470 Ma. The rest of the zircons from the Bjorne Formation yield Precambrian ages. Age peaks are evident at 1216, 1662, 1769, 1933, and 1988 Ma. In addition, ten grains have ages between 2380 and 2940. The Ordovician and 1216 Ma age peaks in the Bjorne Formation are similar to those in the Ledge Sandstone Member of the Ivashak Formation in the Sadlerochit Mountains, but otherwise this sample is very different in that it has an absence of Cambrian and Late Precambrian ages and far more older Precambrian zircons (Figure 6). Given the inferred SE source for the Bjorne Formation (including the Canadian Shield), the older ages are easily explained. However, this sample stands out in our data set because its source areas are so different from the other circum-Arctic sandstones discussed so far. Sample AE-1 does have similarities to the pattern of detrital zircon ages reported for two samples of Carboniferous sandstones from the Outer Moray Firth in the northern part of the North Sea [*Morton et al.*, 2001] emphasizing the distinction between Siberian and Laurasian-European detrital sources.

5. Conclusions

[30] The reconnaissance nature of this study and the immense size of the region sampled make it difficult to make unequivocal conclusions based on the few data discussed in this paper; rather, the inferences from these data as listed below represent testable hypotheses. More data from key stratigraphic sections is the next step needed to build on these initial inferences. The fact that many of the potential source areas for the sediments we have studied are not themselves geochronologically well characterized presents additional problems in interpreting the data. Despite this, the new data provide a powerful means of comparing source regions for Triassic sediments and must

be used for testing any existing or proposed plate tectonic models for the Arctic.

[31] When all the data are considered together (Figure 6), the following general conclusions can be made:

[32] 1. The three samples of Triassic sandstone deposited along the northern Verkhoyansk margin (locality 1, Figures 1, 2, and 3) have distinctive detrital populations represented mainly by Permo-Caboniferous and Cambro-Ordovician-Silurian age zircons (Figure 5). Late Precambrian (1000 to 1315 Ma) zircons, which are present in all other samples studied, are conspicuously absent. Cambrian-latest Precambrian zircons (500 to 750 Ma), although present, are of lesser importance. The stratigraphy, sedimentology and petrology of the Triassic of the Verkhoyansk are quite well known, as is the concept that they were derived from actively uplifting mountain systems in the Baikal region via a system of large rivers that delivered siliciclastic debris to the Verkhoyansk margin from Carboniferous to Jurassic time. The detrital zircon populations support this inference; specifically, there is a good match in the detrital zircon ages with the known age of the extensive Angara-Vitim batholith of Permo-Carboniferous age (290–320 Ma) in the Baikal mountainous region.

[33] 2. The three samples from Chukotka and one from Wrangel Island (localities 2 and 3, Figure 1) are from strata that are the least studied stratigraphically and sedimentologically. Their zircon populations are very similar. They are distinct from those of the Verkhoyansk because they contain Permo-Triassic and 1000–1315 Ma zircons. Permo-Carboniferous and Ordovician age peaks are similar to those in the Verkhoyansk. Chukotka and Wrangel detrital zircon suites are more like the Verkhoyansk and are dissimilar from Canadian and eastern Alaska samples. Like the Verkhoyansk, the Triassic sediments of Chukotka are derived from orogenic source regions. The source region for Permo-Triassic zircons in Chukotka was most likely the Taimyr region and/or zircon-bearing magmas related to the Siberian Traps. If so, it is likely that Permo-Carboniferous sources in the Taimyr region dated at 264–300 Ma may have provided zircons to these sediments as well. These ages preclude Laurentian sources because the Greenland and Canada Caledonides do not have magmatic belts that are this young (post-350 Ma) [e.g., *Currie*, 1995; *Torsvik and Cocks*, 2004]. Since Ordovician age peaks are present in all samples dated, it is perhaps coincidental that Verkhoyansk and Chukotka samples have similar Permo-Carboniferous and Ordovician peaks, but without further work, a Baikal Mountains source (or recycled source) cannot be ruled out for the Triassic of Chukotka, provided the Taimyr and Siberian Trap region of Russia are also included as parts of that source region. Similar orogenic histories to those of the Baikals occur within the Ural Mountains of Russia [*Khain and Nikishin*, 1997] and thus river systems that drained the northern Urals, provided they included the Taymir region/Siberian Traps, would also represent a feasible source region. In addition, Chukotka's history of rifting in the Triassic is unique to this part of the Arctic Alaska-Chukotka microplate and must be taken into account in any paleogeographic reconstruction.

[34] 3. Triassic sandstones from the Lisburne Hills of western Alaska (locality 4, Figures 1 and 3) have similar zircon populations to those of Chukotka and Wrangel Island, suggesting no significant paleogeographic barriers between the Russian and westernmost Alaskan parts of the Arctic Alaska-Chukotka microplate in the Triassic, despite significant differences in facies and thicknesses. Specifically, Triassic sandstones from both these regions share Permo-Triassic and Permo-Carboniferous age detrital zircons. In addition to having Ordovician, Cambrian-Late Precambrian and some 1000 to 1300 Ma age zircons in common, the Chukotka and western Alaska samples also share Devonian age peaks. Devonian granitoids have been dated in multiple localities in Alaska and Chukotka, where they intrude rocks that are basement to Mississippian and younger sediments.

[35] 4. The greatest difference in detrital zircon populations noted within the Arctic Alaska-Chukotka microplate is found by comparing Triassic sandstones from western versus eastern Alaska, or across a region that has been well studied and is known for its structural and stratigraphic continuity. Permo-Triassic and Permo-Carboniferous sources are not represented in samples from the Triassic of the Sadlerochit Mountains in eastern Alaska (locality 5, Figure 1). Instead, Ordovician (445–490 Ma) and Cambrian-latest Precambrian (500–600 Ma) zircons predominate. In addition, 900–1000 and 1000–1300 Ma age zircons are also present. Thus there is good evidence for along-strike changes in provenance for Triassic sandstones of the Arctic Alaska-Chukotka microplate across Alaska.

[36] 5. The Upper Triassic Pat Bay Formation of the Sverdrup Basin, Arctic Canada (locality 6, Figure 1), was derived from a northern source region that is no longer present because it was rifted away during opening of the Amerasian Basin. Our one sample from the Pat Bay Formation yielded a detrital zircon population that is nearly identical to that of the sample from the Sadlerochit Mountains. The now missing "Crockerland" of *Embry* [1992] appears to have sourced both these region in the Late Triassic and must have been characterized by igneous or sedimentary rocks containing mostly 500–600 Ma zircons, with less important Ordovician and late Precambrian sources represented.

[37] 6. The Lower Triassic Bjorne Formation of the Sverdrup Basin (locality 7, Figure 1) is known to have been derived from the south margin of the Sverdrup Basin, and its detrital zircon population is quite different from that of the Pat Bay Formation. It reflects a 430–470 Ma source, but has no zircons in the 500–600 Ma range. Instead it is dominated by 1130–1240 Ma and older Precambrian zircons. This data is compatible with the inference that rivers that fed sediment to the Bjorne Formation from the south contained detritus eroded from the Canadian Shield as well as from the Caledonides [*Embry*, 1992].

6. Discussion

[38] The above conclusions and inferences from data are used to evaluate paleogeographic and plate tectonic recon-

structions for the Arctic Ocean. First we consider the accepted reconstruction shown in Figure 2 [after *Lawver et al.*, 2002], which is similar to that of *Rowley and Lottes* [1988]. *Rowley and Lottes'* [1988] reconstruction has no overlap of continental crust like that depicted in Figure 2. This was accomplished by not including the New Siberian Islands and surrounding Siberian Shelf as part of the Arctic Alaska-Chukotka microplate. However, geologic work on the New Siberian Islands [e.g., *Kuzmichev and Soloviev*, 2004] and aeromagnetic data from the shelf [*Racey et al.*, 1996] argues that the Late Jurassic–Early Cretaceous fold and thrust belt with accreted ophiolitic terranes includes the New Siberian Islands. An additional problem with the ''rotational model'' is that it restores a well-developed Mesozoic orogenic belt with accreted oceanic and arc terranes (the Brooks Range–Chukotka orogen) against the platformal region of the Barents Shelf (Figure 2). The ''rotational model'' restores Chukotka to a position where it is separated from potential sedimentary source areas in NE Russia by a 1000-km-wide ocean (Figure 2). Yet our data suggests that these sources played an important role in providing sediment to Triassic basins of Chukotka, Wrangel Island and westernmost Alaska. Furthermore, Chukotka restores to a position adjacent to the north rim of the Sverdrup Basin, whose source regions for Triassic sandstones are the most dissimilar to those represented by zircons in Triassic sandstones of Wrangel Island and Chukotka (Figure 6).

[39] Figure 7 illustrates a highly schematic paleogeographic reconstruction of the Arctic Alaska-Chukotka microplate that better satisfies both the geologic data and our new sedimentologic constraints. The base map is the Early Albian (110 Ma) reconstruction of *Rowley and Lottes* [1988] and shows the North Atlantic closed and the Lomonosov Ridge as part of the Barents Shelf. The International Bathymetric Chart of the Arctic Oceans (IBCAO, 2001, available at http://www.ngdc.noaa.gov/mgg/bathymetry/arctic/arctic.html) is shown as base for the Amerasian Basin to highlight the position and nature of intrabasinal highs that must be considered. These include the continental Chukchi Borderland [*Grantz et al.*, 1990a] and the Alpha and Mendeleev ridges of more questionable origin. We have mapped linear normal faults associated with the intrabasinal highs of the Arctic Ocean (Figure 7a). The structuring of these intrabasinal highs is compatible with the interpretation that the Alpha and Mendeleev highs are stretched and foundered continental crust rather than a younger hot spot track [*Lawver and Müller*, 1998]. The extensional structures of the Alpha Mendeleev Ridge have been documented by the sparse reflection seismic data available [*Jackson et al.*, 1990; *Jokat*, 2003; *Coakley et al.*, 2005] and gravity models suggest a 20–30 km thick crust in places beneath the Alpha-Mendeleev Ridge [*Williams and Coakley*, 2005] supporting the interpretation that it is underlain by thinned continental crust. The orientation of the various arrays of normal faults (ridges and basins) seen in the bathymetric data suggest a complex mode of stretching and opening for this part of the Amerasian Basin, with both rifting parallel to the Lomonosov Ridge and orthogonal to the Canadian margin (Figure 7a). A rift origin for the Makarov Basin, located between the Lomonosov and Alpha Mendeleev ridges, was initially proposed [e.g., *Taylor et al.*, 1981; *Vogt et al.*, 1982] and is supported by the parallel systems of horsts and grabens along its border with the Lomonosov Ridge [*Cochran et al.*, 2003] (Figure 7a). However, the expected parallel magnetic anomalies are not observed in the aeromagnetic data [e.g., *Brozena et al.*, 2002].

[40] Triassic paleogeographic features of the circum-Arctic are schematically shown in Figure 7a and include possible major sources of sediment supply from Eurasia, today's outcrop region of the Siberian Trap basalts, the failed rift system beneath the West Siberian Basin [e.g., *Aplonov*, 1988; *Ziegler*, 1988], and the inferred sediment source directions for Alaskan and Canadian sample sites. Within the Arctic Alaska-Chukotka microplate, we have outlined the approximate northern boundary of Late Jurassic–Early Cretaceous ''Brookian'' thrust faulting and the location of the Angayucham, South Anyui and Kolyma-Verkhoyansk ophiolite/arc collision boundaries. These features formed prior to the opening of the Amerasian Basin and constitute good markers or piercing points for pre-Cretaceous reconstruction.

[41] The pre-Cretaceous reconstruction (Figure 7b) places Chukotka close to the Taimyrs and Siberian Traps, satisfying the source region constraints provided by detrital zircon suites. It also places Chukotka closer to possible prolongations of the West Siberian Rift system. During its time of formation, the branches of this rift system may have hosted river systems that could have transported sediments from great distances across Siberia into the Triassic rift basins of Chukotka. These sediment sources could have included Permo-Triassic zircons from the Taimyr and Siberian Trap region as well (Figure 7b).

[42] In order to restore Chukotka to its prerift location (Figure 7b), several assumptions were required:

[43] 1. The Arctic Alaska-Chukotka microplate is not a rigid crustal fragment. This is supported by extensive data from the Bering Strait region [*Klemperer et al.*, 2002] and a growing database from Chukotka [*Katkov et al.*, 2004, 2005] that suggests extensional deformation during the time span of Cretaceous magmatism (120–90 Ma). The reconstruction (Figure 7b) breaks the microplate arbitrarily in the Bering Strait, despite the fact that many geological elements seem to be present on both sides of the strait (Figure 3).

[44] 2. The East Siberian Shelf has undergone ~100% extension (doubling in width) in an approximately EW direction. Gravity and limited seismic data support this assumption [e.g., *Drachev*, 2004] and at least this amount of extension is required if assumption 3 is valid.

[45] 3. The highs in the Amerasian Basin are composed of thinned continental crust that restore to form part of the Lomonosov Ridge–Barents Shelf, helping to provide extra continental crust needed to fill the gap between the microplate and the rifted edge of the Barents Shelf.

[46] The resulting paleogeography of the Arctic (Figure 7b) appears substantially different from that of Figure 2 and is testable by the acquisition of additional data.

[47] In summary, the new data presented here on source areas for Triassic sediments in the circum-Arctic show that Siberian, not Laurasian sources are most likely for Triassic sandstones of the Arctic Alaska-Chukotka microplate. This requires revision of the existing "rotational opening model" for the Amerasian Basin of the Arctic Ocean. The new data argue that, while it is reasonable to restore the margin of northern Alaska against the Canadian Arctic Islands, the Chukotka part of the Arctic Alaska-Chukotka microplate must originate closer to Russia in order to receive the sediments that fill its Triassic rift basins. An appropriate pre-Cretaceous location for Chukotka might be outboard of the prolongation of the West Siberian rift system, which underlies the West Siberian Basin (Figure 7). Arctic Canada and Arctic Alaska, especially eastern Alaska, have different sedimentary source regions. Grenville age basement (1000–1300 Ma) in the reconstructed North Atlantic region crosses the Barents Shelf and is present on Svalbard [*Harland*, 1998] and in Pearya, northernmost Ellesmere Island [*Trettin*, 1991]. Igneous and metamorphic events dated at 500–600 Ma are also present in both these localities [e.g., *Trettin*, 1991]. Together with the now foundered remains of the Barents platformal region (such as the continental Lomonosov Ridge and the thinned continental crust of the Alpha-Mendeleev Ridge and the Chukchi Borderland), this region could have constituted part of the now missing "Crockerland" of *Embry* [1992] that supplied zircons to Triassic sediments of eastern Alaska and the northern Sverdrup Basin.

[48] We suggest that the formation of the Amerasian Basin and translation of the Arctic Alaska microplate is far more complex than previously supposed. A large amount of internal deformation of the Arctic Alaska-Chukotka microplate is suspected. Although we are reasonably confident of the most likely pre-Cretaceous position of Arctic Alaska-Chukotka, the kinematics of the opening of the Amerasian Basin remain problematic. A precise solution awaits deep-sea drilling of the basin floor and geophysical and geological studies of its margins.

[49] **Acknowledgments.** This work builds on fieldwork and sampling in Arctic Russia and Alaska funded by NSF (Continental Dynamics EAR93-17087), ExxonMobil, the Department of Geological Sciences at Stanford and Stanford University's School of Earth Science McGuee funds. Special thanks to Steve Creaney, Mike Sullivan, Bob Ferderer, Ian Norton, and Pinar Ilmaz of ExxonMobil for their interest in Arctic tectonics. Thanks to Alexander Kusmichev for a critical early reading of the manuscript and his many insights into the geology of Arctic Russia. Thank you David Rowley and Warren Nokleberg for very helpful reviews.

References

Amato, J. M. (2004), Crystalline basement ages, detrital zircon ages and metamorphic ages from Seward Peninsula: Implications for Proterozoic and Cambrian-Ordovician paleogeographic reconstructions of the Arctic Alaska terrane, *Geol. Soc. Am. Abstr. Programs*, *36*(5), 22.

Amato, J. M., E. L. Miller, and G. E. Gehrels (2003), Lower Paleozoic through Archean detrital zircon ages from metasedimentary rocks of the Nome Group, Seward Peninsula, Alaska, *Eos Trans. AGU*, *84*(46), Fall Meet. Suppl., Abstract T31F-0891.

Andrianova, V. A., and V. N. Andrianov (1970), Nekotorye novye dannye o vulcanisme na rubezhe permskogo I triasovogo periodov v oblasti Verkoyanskoy geosynklinali (Some new data on volcanism during the latest Permian to earliest Triassic timespan in the Verkoyansk geosyncline), *Mater. Geol. Pol. Iskopaemym Yakutskoy ASSR (Contrib. Geol. Miner. Deposits Yakut ASSR)*, *XVI*, 137–145.

Aplonov, S. (1988), An aborted Triassic Ocean in west Siberia, *Tectonics*, *7*, 1103–1122.

Bea, F., G. B. Fershtater, and P. Montero (2002), Granitoids of the Uralides: Implications for the evolution of the orogen, in *Mountain Building in the Uralides: Pangea to the Present*, *Geophys. Monogr. Ser.*, vol. 132, edited by D. Brown, C. Juhlin, and V. Puchkov, pp. 211–232, AGU, Washington, D. C.

Belik, G. Y., and G. M. Sosunov (1969), Geologic map of USSR: Anyuisko-Chaunskaya series, *Map R-58–XXIX, XXX*, scale 1:200,000, North-East. Geol. Dir., Magadan, Russia.

Blome, C. D., K. M. Reed, and I. L. Tailleur (1988), Radiolarian biostratigraphy of the Otuk Formation in and near the National Petroleum Reserve in Alaska, in *Geology and Exploration of the National Petroleum Reserve in Alaska, 1974 to 1982*, edited by G. Gryc, *U.S. Geol. Surv. Prof. Pap.*, *1399*, 725–776.

Brozena, J. M., L. A. Lawver, L. C. Kovacs, and V. A. Childers (2002), Aerogeophysical evidence for the rotational opening of the Canada Basin, *AAPG Bull.*, *86*, 1138.

Bukharov, A. A., V. A. Khalilov, T. M. Strakhova, and V. V. Chernikov (1992), Geology of the Baikal-Patom Upland according to new data of U-Pb dating, *Russ. Geol. Geophys.*, *33*, 24–33.

Bychkov, Y. M. (1994), Structural-facies zonation and biostratigraphy of the Triassic in Chukotka (in Russian), 53 pp., Northeast Sci. Centre, Magadan.

Bychkov, Y. M., and M. E. Gorodinsky (1992), Comparative geology of northern Chukotka and the northern Canadian Cordillera, paper presented at International Conference on Arctic Margins, U.S. Dep. of Inter., Miner. Manage. Serv., Anchorage, Alaska.

Campbell, I. H., G. K. Czamanske, V. A. Fedorenko, R. I. Hill, and V. Stepanov (1992), Synchronism of the Siberian traps and the Permian-Triassic boundary, *Science*, *258*, 1760–1763.

Chasovitin, M. D., and A. P. Shpetnyi (1964), Geologic map of USSR: Anyuisko-Chaunskaya series, *Map R-58–XXXIII, XXXIV*, scale 1:200,000, North-East. Geol. Dir., Magadan, Russia.

Coakley, B., et al. (2005), A cross-Arctic geophysical transect collected from US Coast Guard Icebreaker Healy, *Eos Trans. AGU*, *86*(52), Fall Meet. Suppl., Abstract T13D-0510.

Cochran, J. R., M. H. Edwards, and B. J. Coakley (2003), Differing forms of continental rifting on the Eurasian and Amerasian margins of the Lomonosov Ridge, Arctic Ocean, *Eos Trans. AGU*, *84*(46), Fall Meeting Suppl., T12A-0450.

Currie, K. L. (1995), Plutonic rocks, in *Geology of Canada*, vol. 6, *Geology of the Appalachian-Caledonian Orogen in Canada and Greenland*, edited by H. Williams, pp. 629–680, Geol. Surv. of Can., Ottawa, Ont.

DeGraaf-Surpless, K., S. A. Graham, J. L. Wooden, and M. C. McWilliams (2002), Detrital zircon provenance analysis of the Great Valley Group, California: Evolution of an arc-fore arc system, *Geol. Soc. Am. Bull.*, *114*, 1564–1580.

Dickinson, W. R., and G. E. Gehrels (2003), U-Pb ages of detrital zircons from Permian and Jurassic eolian sandstones of the Colorado Plateau U.S.A.: Paleogeographic implications, *Sediment. Geol.*, *163*, 29–66.

Drachev, S. S. (2004), Siberian Arctic continental margin: Constraints and uncertainties of plate tectonic models, *Eos Trans. AGU*, *85*(47), Fall Meet. Suppl., Abstract GP43C-07.

Dumoulin, J. A., A. G. Harris, M. Gagiev, D. C. Bradley, and J. E. Repetski (2002), Lithostratigraphic, conodont, and other faunal links between lower Paleozoic strata in northern and central Alaska and northeastern Russia, in *Tectonic Evolution of the Bering Shelf-Chukchi Sea-Arctic Margin and Adjacent Landmasses*, edited by E. L. Miller, A. Grantz, and S. L. Klemperer. *Spec. Pap. Geol. Soc. Am.*, *360*, 291–312.

Embry, A. F. (1991), Mesozoic history of the Arctic Islands, in *The Geology of Canada*, vol. 3, *Geology of the Innuitian Orogen and Arctic Platform of Canada and Greenland*, edited by H. P. Trettin, pp. 371–434, Geol. Surv. of Can., Ottawa, Ont.

Embry, A. F. (1992), Crockerland-the northwest source for the Sverdrup Basin, Canadian Arctic Islands, in *Arctic Geology and Petroleum Potential*, *NPF Spec. Publ.*, vol. 2, edited by T. O. Vorren et al., pp. 205–216, Elsevier, New York.

Embry, A. F., and J. Dixon (1990), The breakup unconformity of the Amerasian Basin, Arctic Ocean: Evidence from Arctic Canada, *Geol. Soc. Am. Bull.*, *102*, 1526–1534.

Gelman, M. L. (1963), Triassic diabase association in the Aniuy fold zone (Chukotka) (in Russian), *Geol. Geofiz.*, *2*, 127–134.

Grantz, A., S. D. May, and P. E. Hart (1990a), Geology of Arctic continental margin of Alaska, in *The Geology of North America*, vol. L, *The Arctic Ocean Region*, edited by A. Grantz, L. Johnson, and J. F. Sweeney, pp. 257–288, Geol. Soc. of Am., Boulder, Colo.

Grantz, A., S. D. May, P. T. Taylor, and L. A. Lawver (1990b), Canada Basin, in *The Geology of North America*, vol. L, *The Arctic Ocean Region*, edited by A. Grantz, L. Johnson, and J. F. Sweeney, pp. 379–402, Geol. Soc. of Am., Boulder, Colo.

Harland, W. B. (1998), *Geology of Svalbard*, *Mem. Geol. Soc. London*, *17*, 529 pp.

Ivanov, O. N., and A. P. Milov (1975), The diabase association in the Chukchi fold system and its relation to the basic magmatism in the northern portion of the Pacific Mobile Belt (in Russian), in *Magmatism of North East Asia, part 2*, edited by E. T. Shatalov, pp. 155–159, Magadan Publ. House, Magadan, Russia.

Jackson, H. R., D. A. Forsyth, J. K. Hall, and A. Overton (1990), Seismic reflection and refraction, in *The Geology of North America*, vol. L, *The Arctic Ocean Region*, edited by A. Grantz, L. Johnson, and J. F. Sweeney, pp. 153–170, Geol. Soc. of Am., Boulder, Colo.

Jokat, W. (2003), Seismic investigations along the western sector of Alpha Ridge, central Arctic Ocean, *Geophys. J. Int.*, *152*, 185–201.

Katkov, S. M., E. L. Miller, I. I. Podgorny, and J. Toro (2004), Deformation history of central Chukotka (Alarmaut Uplift) northeastern Arctic Russia, *Eos Trans. AGU*, *85*(47), Fall Meet. Suppl., Abstract GP41A-0813.

Katkov, S. M., A. Strickland, E. L. Miller, I. I. Podgorny, and J. Toro (2005), Dating deformation in the Anyui-Chukotka fold belt, northeastern Arctic Russia, *Eos Trans. AGU*, *85*(47), Fall Meet. Suppl. Abstract T11B-0378.

Khain, V. E., and A. Nikishin (1997), Russia, in *Encyclopedia of European and Asian Regional Geology*, edited by E. M. Moores and R. W. Fairbridge, pp. 631–653, CRC Press, Boca Raton, Fla.

Khudoley, A. K., and G. A. Guriev (1994), The formation and development of a late Paleozoic sedimentary basin on the passive margin of the Siberian paleocontinent, in *Pangea: Global Environments and Resources*, edited by A. F. Embry, B. Beauchamp, and D. J. Glass, *Mem. Can. Soc. Pet. Geol.*, *17*, 131–143.

Klemperer, S. L., E. L. Miller, A. Grantz, D. W. Scholl, and The Bering-Chukchi Working Group (2002), Crustal structure of the Bering and Chukchi shelves: Deep seismic reflection profiles across the North American continent between Alaska and Russia, in *Tectonic Evolution of the Bering Shelf–Chukchi Sea–Arctic Margin and Adjacent Landmasses*, edited by E. L. Miller, A. Grantz, and S. L. Klemperer, *Spec. Pap. Geol. Soc. Am.*, *360*, 1–24.

Kos'ko, M. K., M. P. Cecile, J. C. Harrison, V. G. Ganelin, N. V. Khandoshko, and B. G. Lopatin (1993), Geology of Wrangel Island, between Chukchi and East Siberian seas, northeastern Russia, *Geol. Surv. Can. Bull.*, *461*, 101 pp.

Kossovskaya, A. G., V. D. Shutov, and V. I. Muravyev (1960), Mesozoic and upper Paleozoic deposits of the West Verkhoyansk Region and the Vilyui Basin, Moscow (in Russian), *Trans. Geol. Inst. Acad. Sci. USSR*, *34*, 276 pp.

Kuzmichev, A. B., and A. V. Soloviev (2004), Mesozoic flysch of the Big Lyakhov Island (New Siberian Islands): Age, provenance and tectonic setting, in *Arctic Geology, Energy Resources and Environmental Challenges*, edited by M. Smelror and T. Bugge, pp. 80–82, Norsk Geol. Forening, Trondheim, Norway.

Lawver, L. A., and R. D. Müller (1998), Iceland hotspot track, *Geology*, *22*, 311–314.

Lawver, L. A., and C. R. Scotese (1990), A review of tectonic models for the evolution of the Canada Basin, in *The Geology of North America*, vol. L., *The Arctic Ocean Region*, edited by A. Grantz, L. Johnson, and J. F. Sweeney, pp. 593–618, Geol. Soc. of Am., Boulder, Colo.

Lawver, L. A., A. Grantz, and L. M. Gahagan (2002), Plate Kinematic evolution of the present Arctic region since the Ordovician, in *Tectonic Evolution of the Bering Shelf-Chukchi Sea-Arctic Margin and Adjacent Landmasses*, edited by E. L. Miller, A. Grantz, and S. L. Klemperer, *Spec. Pap. Geol. Soc. Am.*, *360*, 333–358.

Laxon, S., and D. McAdoo (1994), Arctic Ocean gravity field derived from ERS-1 satellite altimetry, *Science*, *265*, 621–624.

Ludwig, K. R. (2003), User's manual for Isoplot 3.0: A geochronological toolkit for Microsoft Excel, *Spec. Pub. 4*, 71 pp., Berkeley Geochronol. Center, Berkeley, Calif.

Mariani, R. K. (1987), Petrography and diagenesis of the Ledge Sandstone member of the Triassic Ivishak Formation, in *Petroleum Geology of the Northern Part of the Arctic National Wildlife Refuge, Northeastern Alaska*, edited by K. J. Bird and L. B. Magoon, *U.S. Geol. Surv. Bull.*, *1778*, 101–115.

Miller, E. L., M. Gelman, L. Parfenov, and J. Hourigan (2002), Tectonic setting of Mesozoic magmatism: A comparison between northeastern Russia and the North American Cordillera, in *Tectonic Evolution of the Bering Shelf-Chukchi Sea-Arctic Margin and Adjacent Landmasses*, edited by E. L. Miller, A. Grantz, and S. L. Klemperer, *Spec. Pap. Geol. Soc. Am.*, *360*, 333–358.

Miller, E. L., J. Toro, G. Gehrels, M. Tuchkova, and S. Katkov (2004), Detrital zircon ages from Late Jurassic–Early Cretaceous Myrgovaam Basin sandstones (Rauchua Trough), western Chukotka, NE Russia, *Eos Trans. AGU*, *85*(47), Fall Meet. Suppl., Abstract GP44A-04.

Moore, T. E., W. K. Wallace, K. J. Bird, S. M. Karl, C. G. Mull, and J. T. Dillon (1994), Geology of northern Alaska, in *The Geology of North America*, vol. G-1, *The Geology of Alaska*, edited by G. Plafker and H. C. Berg, pp. 49–140, Geol. Soc. of Am., Boulder, Colo.

Moore, T. E., T. A. Dumitru, K. E. Adams, S. N. Witebsky, and A. G. Harris (2002), Origin of the Lisburne Hills-Herald Arch structural belt: Stratigraphic, structural and fission track evidence from the Cape Lisburne area, northwestern Alaska, in *Tectonic Evolution of the Bering Shelf-Chukchi Sea-Arctic Margin and Adjacent Landmasses*, edited by E. L. Miller, A. Grantz, and S. L. Klemperer, *Spec. Pap. Geol. Soc. Am.*, *360*, 77–109.

Morton, A. C., J. C. Claoue-Long, and C. R. Hallsworth (2001), Zircon age and heavy mineral constraints on provenance of North Sea Carboniferous sandstones, *Mar. Pet. Geol.*, *18*, 319–337.

Natal'in, B. A. (2004), Phanerozoic tectonic evolution of the Chukotka-Arctic Alaska Block: Problems of the rotational model, *Eos Trans. AGU*, *85*(47), Fall Meet. Suppl., Abstract GP43C-04.

Natal'in, B. A., J. M. Amato, J. Toro, and J. E. Wright (1999), Paleozoic rocks of northern Chukotka Peninsula, Russian Far East: Implications for the tectonics of the Arctic region, *Tectonics*, *18*, 977–1003.

Oxman, V. S., L. M. Parfenov, A. V. Prokopiev, V. F. Timofeev, F. F. Tretyakov, Y. D. Nedosekin, P. W. Layer, and K. Fujita (1995), The Chersky Range ophiolite belt, northeast Russia, *J. Geol.*, *103*, 539–557.

Pease, V., and V. Vernikovsky (2000), The tectonomagmatic evolution of the Taimyr Peninsula: Further constraints from new ion-microprobe data, *Polarforschung*, *68*, 1–3.

Pease, V., D. G. Gee, V. Vernikovsky, A. Vernikovskaya, and S. Kireev (2001), Geochronology and magmatic and metamorphic events in central Taimyr, northern Siberia, *Terra Nova*, *13*, 270–280.

Polae, V. P. (1966), Gosudarstvennaya geologicheskaya karta SSSR (National Geological map of USSR), 1:200,000 scale, Chukotsk series, Sheet R-60–XXIX, XXX, XXIII, XXIV, MinGeo Russ., Moscow.

P'yankov, A. Y. (1981), Gosudarstvennaya geologicheskaya karta SSSR (National Geological map of USSR), 1:200,000 scale, Anyui-Chaun series, Sheet R-60–XXI, XXII, MinGeo Russ., Magadan.

P'yankov, A. Y., and T. P. Huppenen (1974), Gosudarstvennaya geologicheskaya karta SSSR (National Geological map of USSR), 1:200,000 scale, Anyui-Chaun series, Sheet R-60–XIX, XX, MinGeo Russ., Moscow.

Racey, S. D., S. J. McLean, W. M. Davis, R. W. Buhmann, and A. M. Hittelman (1996), Magnetic anomaly data of the former Soviet Union, version 1.0 [CD-ROM], NOAA, Natl. Geophys. Data Center, Boulder, Colo.

Renne, P. R., and A. R. Basu (1996), Rapid eruption of the Siberian traps flood basalts at the Permo-Triassic boundary, *Science*, *253*, 176–179.

Rowley, D. B., and A. L. Lottes (1988), Plate kinematic reconstructions of the North Atlantic and Arctic: Late Jurassic to Present, *Tectonophysics*, *155*, 73–120.

Rubatto, D., I. S. Williams, and I. S. Buck (2001), Zircon and monazite response to prograde metamorphism in the Reynolds Range, central Australia, *Cont. Mineral. Petrol.*, *140*, 458–468.

Scarrow, J. H., R. Hetzel, V. M. Gorozhanin, M. Dinn, J. Glodny, A. Gerdes, C. Ayala, and P. Montero (2002), Four decades of geochronological work in the southern and middle Urals; a review, in *Mountain Building in the Uralides: Pangea to the Present*, *Geophys. Monogr. Ser.*, vol. 132, edited by D. Brown, C. Juhlin, and V. Puchkov, pp. 233–255, AGU, Washington, D. C.

Sengor, A. M. C., and B. A. Natalin (2004), Tectonics of the Altaids: An example of a Turkic-type orogen, in *Earth Structure*, edited by B. A. Van der Pluijm and S. Marshak, pp. 535–546, Norton, New York.

Seslavinskiy, K. B. (1979), The south Anyui suture (western Chukotka) (in Russian), *Dokl. Akad. Nauk SSSR*, *249*, 1181–1185.

Sherwood, K. W., P. P. Johnson, J. D. Craig, S. A. Zerwick, R. T. Lothamer, D. K. Thurston, and S. B. Hurlbert (2002), Structure and stratigraphy of the Hanna Trough, U.S. Chukchi Shelf, Alaska, in *Tectonic Evolution of the Bering Shelf–Chukchi Sea–Arctic Margin and Adjacent Landmasses*, edited by E. L. Miller, A. Grantz, and S. L. Klemperer, *Spec. Pap. Geol. Soc. Am.*, *360*, 39–66.

Sokolov, S. D., G. Y. Bondarenko, O. L. Morozov, V. A. Shekhovtsov, S. P. Glotov, A. V. Ganelin, B. Kravchenko, and I. R. Berezhnoy (2002), South Anyui suture, Northeast Arctic Russia; facts and problems, in *Tectonic Evolution of the Bering Shelf–Chukchi Sea–Arctic Margin and Adjacent Landmasses*, edited by E. L. Miller, A. Grantz, and S. L. Klemperer, *Spec. Pap. Geol. Soc. Am.*, *360*, 209–224.

Sosunov, G. M., and S. M. Til'man (1960), Geologic map of USSR, Anyuisko-Chaunskaya series, *Map R-58–XXXV. XXXVI*, scale 1:200,000, North-East. Geol. Dir., Magadan, Russia.

Stacey, J., and J. Kramers (1975), Approximation of terrestrial lead isotope evolution by a two-stage model, *Earth Planet. Sci. Lett.*, *26*, 207–221.

Taylor, P. T., L. C. Kovacs, P. R. Vogt, and G. L. Johnson (1981), Detailed aeromagnetic investigation of the Arctic Basin, *J. Geophys. Res.*, *86*, 6323–6333.

Tolson, R. B. (1987), Structure and stratigraphy of the Hope Basin, southern Chukchi Seas, Alaska, in *Geology and Resource Potential of the Continental Margin of Western North America and Adjacent Ocean Basins—Beaufort Sea to Baja California*, *Earth Sci. Ser.*, v. 6, edited by D. W. Scholl, A. Grantz, and J. G. Vedde, pp. 59–71, Circum-Pac. Counc. for Energy and Miner. Resour., Houston, Tex.

Toro, J., P. B. Gans, W. B. McClelland, and T. Dumitru (2002), Deformation and exhumation of nappes in the Mt. Igikpak region, central Brooks Range, Alaska, in *Tectonic Evolution of the Bering*

Shelf–Chukchi Sea–Arctic Margin and Adjacent Landmasses, edited by E. L. Miller, A. Grantz, and S. L. Klemperer, *Spec. Pap. Geol. Soc. Am.*, *360*, 111–132.

Toro, J., F. Toro, K. J. Bird, and C. Harrison (2004), The Arctic Alaska-Canada connection revisited, *Geol. Soc. Am. Abstr. Programs*, *36*, 22.

Torsvik, T. H., and L. M. R. Cocks (2004), Earth geography from 400 to 250 million years: A palaeomagnetic, faunal and facies review, *J. Geol. Soc. London*, *161*, 555–572.

Trettin, H. P. (1991), The Proterozoic to Late Silurian record of Pearya, in *The Geology of Canada*, vol. 3, *Geology of the Innuitian Orogen and Arctic Platform of Canada and Greenland*, edited by H. P. Trettin, pp. 241–259, Geol. Surv. of Can., Ottawa, Ont.

Tuchkova, M. I., G. Y. Bondarenko, E. L. Miller, and S. M. Katkov (2004), Triassic terrigeneous deposits of western Chukotka: Sedimentation, mineral composition, deformations (NE Russia), *Eos Trans. AGU*, *85*(47), Fall Meet. Suppl., Abstract GP41A-0816.

Venkatesan, T. R., A. Kumar, K. Gopolan, and A. I. Al'mukhamedov (1997), $^{40}Ar/^{39}Ar$ age of Siberian basaltic volcanism, *Chem. Geol.*, *138*, 303–310.

Vernikovsky, V. A. (1996), Geodymamic evolution of the Taimyr folded area (in Russian), 202 pp., United Inst. of Geol., Geophys., and Mineral., Siberian Br., Russ. Acad. of Sci., Novosibirsk, Russia.

Vernikovsky, V. A., E. B. Salanikova, A. B. Kotov, V. P. Kovach, and S. Z. Yakovleva (1988), Precambrian granites of the Faddey terrane (northern Taimyr): New geochemical and geochronological (U-Pb, Sm-Nd) data (in Russian), *Dokl. Russ. Akad. Nauk*, *363*, 653–657.

Vernikovsky, V. A., V. L. Pease, A. E. Vernikovskaya, A. P. Romanov, D. G. Gee, and A. V. Travin (2003), First report of early Triassic A-type granite and syenite intrusions from Taimyr: Product of the northern Eurasian superplume?, *Lithos*, *66*, 23–36.

Vogt, P. R., P. T. Taylor, L. C. Kovacs, and G. L. Johnson (1982), The Canada Basin: Aeromagnetic constraints on structure and evolution, *Tectonophysics*, *89*, 295–336.

Wickham, S. M., B. A. Litvinovsky, A. N. Zanvilevich, and I. N. Bindeman (1995), Geochemical evolution of Phanerozoic magmatism in Transbaikalia, East Asia; a key constraint on the origin of K-rich silicic magmas and the process of cratonization, *J. Geophys. Res.*, *100*, 15,641–15,654.

Williams, C. C., and B. Coakley (2005), Spectral analysis and isostasy of the Alpha-Mendeleev Ridge, Arctic Ocean, *Eos Trans. AGU*, *85*(47), Fall Meet. Suppl., Abstract T13D-0496.

Williams, I. S. (2001), Response of detrital zircon and monazite, and their U-Pb isotopic systems, to regional metamorphism and host-rock partial melting, Cooma complex, southeastern Australia, *J. Earth Sci.*, *48*, 557–580.

Yarmolyuk, V. V., V. I. Kovalenko, A. B. Kotov, and E. B. Sal'nikova (1997), The Angara-Vitim batholith: On the problem of batholith geodynamics in the central Asia foldbelt, *Geotectonics*, *31*, 359–373.

Zheltovski, V. G. (1976), Gosudarstvennaya geologicheskaya karta SSSR (National Geological map of USSR), 1:200,000 scale, Anyui-Chaun series, Sheet R-60– XXVII, XXVIII, MinGeo Russ., Magadan.

Zhuravlev, G. F. (1976), Gosudarstvennaya geologicheskaya karta SSSR (National Geological map of USSR), 1:200,000 scale, Anyui-Chaun series, Sheet R-60–XXV, XXVI, MinGeo, Russ., Magadan.

Ziegler, P. A. (1988), Evolution of the Arctic–North Atlantic and the western Tethys, *AAPG Mem.*, *43*, 198 pp.

V. V. Akinin, NEISRI, Russian Academy of Sciences, Portovaya 16, Magadan 685000, Russia. (petrol@neisri.magadan.ru)

J. M. Amato, Department of Geological Sciences, MSC 3AB P.O. Box 30001, New Mexico State University, Las Cruces, NM 88003, USA. (amato@nmsu.edu)

M. P. Cecile, Geological Survey of Canada, 3303 33rd Street NW Calgary, AB, Canada T2L 2A7. (mcecile@nrcan.gc.ca)

T. A. Dumitru and E. L. Miller, Department of Geological and Environmental Sciences, Stanford University, Blvd. 320, Stanford, CA 94305, USA. (trevor@pangea.stanford.edu; miller@pangea.stanford.edu)

G. Gehrels, Department of Geosciences, University of Arizona, Tucson, AZ 85721, USA. (ggehrels@geo.arizona.edu)

T. E. Moore, U.S. Geological Survey, MS 901, 345 Middlefield Road, Menlo Park, CA 94025, USA. (tmoore@usgs.gov)

A. Prokopiev, Diamond and Precious Metal Geology Institute, Siberian Branch, Russian Academy of Sciences, 39 Lenin Av., Yakutsk, 677980, Russia. (prokopiev@diamond.ysn.ru)

J. Toro, Department of Geology and Geography, 425 White Hall, P.O. Box 6300, West Virginia University, Morgantown, WV 26506, USA. (jtoro@wvu.edu)

M. I. Tuchkova, Geological Institute, Russian Academy of Sciences, Pyzhevsky 7, Moscow 119017, Russia. (tuchkova@ginras.ru)